

Accepted Manuscript

Synthesis and biological evaluation of novel Ani9 derivatives as potent and selective ANO1 inhibitors

Yohan Seo, Jinhwang Kim, Jiwon Chang, Seong Soon Kim, Wan Namkung, Ikyon Kim



PII: S0223-5234(18)30864-X

DOI: [10.1016/j.ejmech.2018.10.002](https://doi.org/10.1016/j.ejmech.2018.10.002)

Reference: EJMECH 10788

To appear in: *European Journal of Medicinal Chemistry*

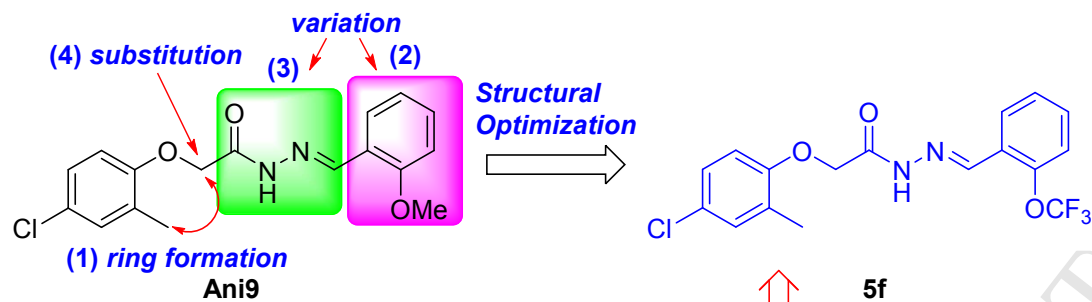
Received Date: 7 August 2018

Revised Date: 18 September 2018

Accepted Date: 1 October 2018

Please cite this article as: Y. Seo, J. Kim, J. Chang, S.S. Kim, W. Namkung, I. Kim, Synthesis and biological evaluation of novel Ani9 derivatives as potent and selective ANO1 inhibitors, *European Journal of Medicinal Chemistry* (2018), doi: <https://doi.org/10.1016/j.ejmech.2018.10.002>.

This is a PDF file of an unedited manuscript that has been accepted for publication. As a service to our customers we are providing this early version of the manuscript. The manuscript will undergo copyediting, typesetting, and review of the resulting proof before it is published in its final form. Please note that during the production process errors may be discovered which could affect the content, and all legal disclaimers that apply to the journal pertain.



- potent ANO1 inhibitor with an IC_{50} value of 22 nM
- excellent selectivity to ANO1 over ANO2 (>1000)
- inhibition of cell proliferation of PC-3, MCF7, and BxPC3 cells expressing high levels of ANO1
- reduction of the level of ANO1 protein expression in PC-3 cells

Synthesis and biological evaluation of novel Ani9 derivatives as potent and selective ANO1 inhibitors

Yohan Seo^{a,b,‡}, Jinhwang Kim^{a,‡}, Jiwon Chang^a, Seong Soon Kim^c, Wan Namkung^{a,b,*}, and
Ikyon Kim^{a,*}

^a College of Pharmacy and Yonsei Institute of Pharmaceutical Sciences, Yonsei University, 85 Songdogwahak-ro, Yeonsu-gu, Incheon, 21983, Republic of Korea

^b Interdisciplinary Program of Integrated OMICS for Biomedical Science Graduate School, Yonsei University, Seoul, 03722, Republic of Korea

^c Bio & Drug Discovery Division, Korea Research Institute of Chemical Technology, Daejeon, 34114, Republic of Korea

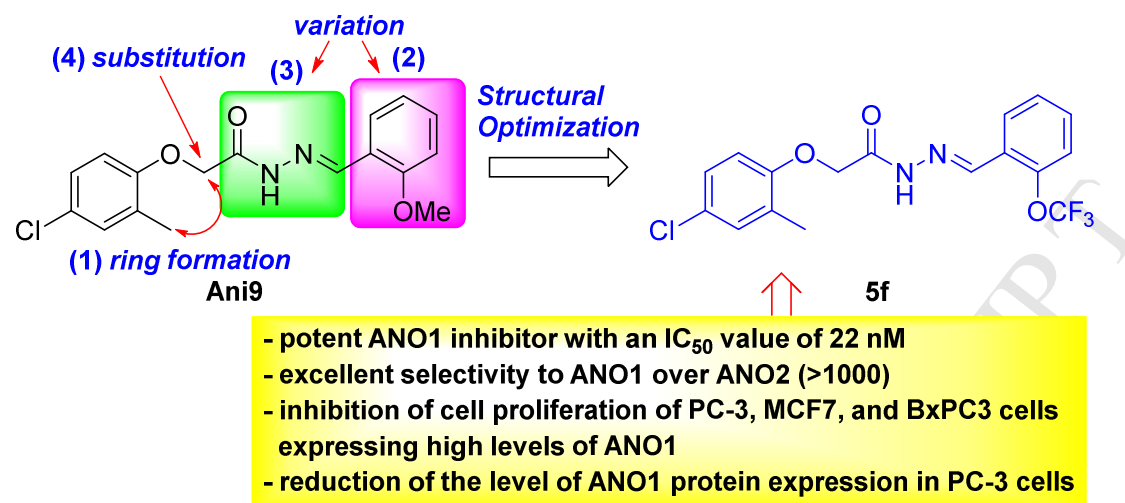
* Corresponding authors.

Tel.: +82 32 749 4519; fax: +82 32 749 4105; e-mail: wnamkung@yonsei.ac.kr

Tel.: +82 32 749 4515; fax: +82 32 749 4105; e-mail: ikyonkim@yonsei.ac.kr

[‡] These authors contributed equally.

Table of Contents



Keywords: Structure-activity relationship; Structural modification; Anoctamin 1 (ANO1); Anil9; Anticancer agent.

Abstract

Anoctamin 1 (ANO1), a calcium-activated chloride channel, is highly expressed and amplified in a number of carcinomas including breast, pancreatic and prostate cancers. Downregulation of ANO1 expression and function significantly inhibits cell proliferation, migration, and invasion of various cancer cell lines. Development of potent and selective ANO1 inhibitors is currently desirable, which may provide a new strategy for cancer treatment. Our previous study revealed a new class of ANO1 inhibitor, (*E*)-2-(4-chloro-2-methylphenoxy)-*N'*-(2-methoxybenzylidene)acetohydrazide (Anil9) and structural optimization via chemical modification of Anil9 basic skeleton was undertaken for the development of more potent and specific inhibitors of ANO1. Structure-activity relationship studies with newly synthesized derivatives revealed a number of potent ANO1 inhibitors,

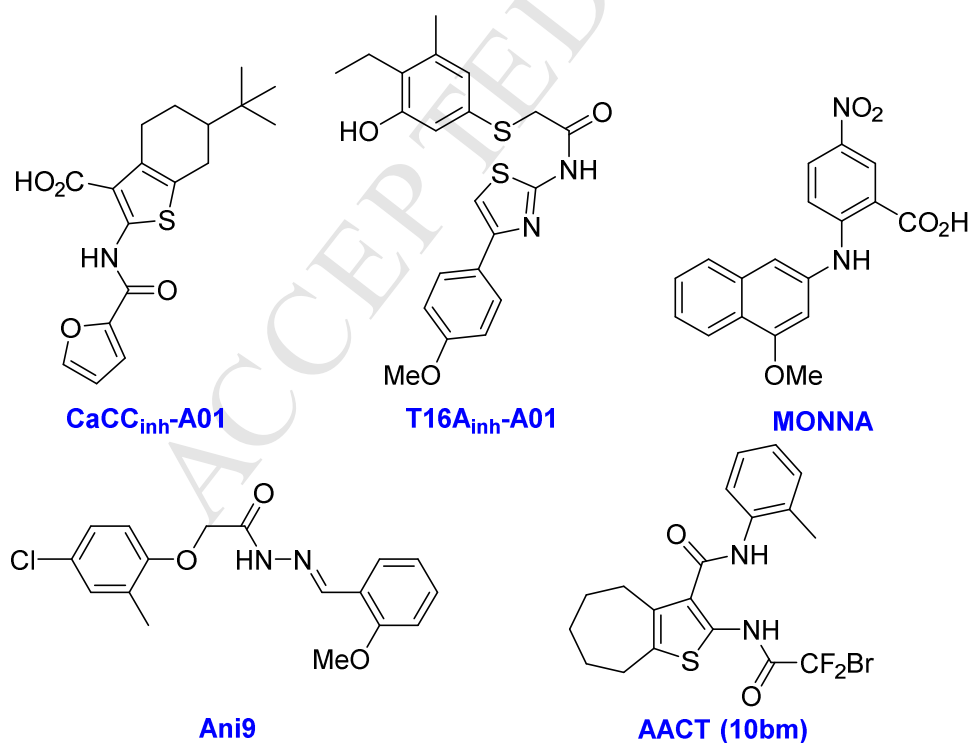
among which **5f** is the most potent inhibitor with an IC_{50} value of 22 nM. The selectivity analyses showed that **5f** has excellent selectivity to ANO1 (>1000-fold over ANO2). In cellular assays, **5f** significantly inhibited cell proliferation of PC3, MCF7, and BxPC3 cells expressing high levels of ANO1. In addition, **5f** strongly reduced the protein levels of ANO1 in PC3 cells. This study will be useful in the development of ANO1 inhibitors for treatment of cancer and other ANO1-related diseases.

Introduction

ANO1, transmembrane member 16A (TMEM16A), is a calcium-activated chloride channel (CaCC) and plays important roles in a wide range of biological processes in various cell types including epithelial cells, smooth muscle cells, intestinal pacemaker cells and sensory neurons [1-4]. In addition, ANO1 is highly expressed and amplified in a variety of carcinomas including breast cancer, pancreatic cancer, prostate cancer, glioblastoma, head-and-neck squamous cell carcinoma (HNSCC) and gastrointestinal stromal tumor (GIST), and play a pivotal role in the regulation of cancer cell proliferation, tumorigenesis and cancer progression [5-11]. Recent evidence suggests that ANO1 inhibitors may have potential utility in treatment of ANO1-related diseases such as inflammatory airway diseases, hypertension and pain [12, 13]. For example, ANO1 inhibition may have a beneficial effect on inflammatory airway diseases via inhibition of excessive mucus secretion in airway epithelium and airway smooth muscle contraction [12]. Inhibition of ANO1 significantly reduced blood pressure in spontaneously hypertensive rats [14, 15]. In an animal model of thermal pain, nocifensive behaviors are significantly decreased by inhibition of ANO1, and capsaicin-mediated pain-related behaviors are also reduced by ANO1 inhibition [16, 17]. In addition, recent studies showed that inhibition of ANO1 by small-molecule inhibitors

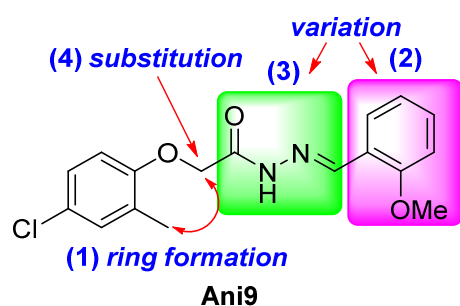
significantly decreased cell proliferation and migration in a wide variety of cancer cell lines including breast, pancreatic and prostate cancer cells expressing high levels of ANO1 [18-21]. ANO1 and ANO2 are verified as CaCCs and share the highest sequence homology among ANO family members [22-24]. ANO2 is highly expressed in olfactory sensory neurons and plays an important role in the regulation of olfactory transduction. Interestingly, recent evidence suggests that ANO2 is involved in reductions of spike generation in thalamocortical and CA1 hippocampal neurons [25, 26], and ANO2 knockout mice show deficits in executive functions and severe impairment in motor learning [27, 28]. Thus, development of selective inhibitors of ANO1 over ANO2 may be a more appropriate therapeutic approach to ANO1-related disease. To date, several small-molecule inhibitors of ANO1 have been identified, including CaCC_{inh}-A01, T16A_{inh}-A01, MONNA, Ani9, and AACT (**10bm**) (Figure 1) [12, 29-32], and Ani9 is the most selective ANO1 inhibitor among the ANO1 inhibitors.

Figure 1. Chemical structures of reported ANO1 inhibitors



With the basic knowledge of Ani9 in hand, we decided to conduct systematic structural optimization via chemical modification of Ani9 to find the more potent ANO1 inhibitor with better selectivity over ANO2, which is the topic of this paper. As shown in Scheme 1, we hoped to synthesize Ani9 derivatives by following the four principles: (1) formation of a ring (2) substitution of 2-methoxyphenyl by different (hetero)aryl moieties (purple region) (3) replacement of the acylhydrazone with different pharmacophores (green region) (4) introduction of substituent(s) at the alpha position of the carbonyl group.

Scheme 1. Synthetic Plan

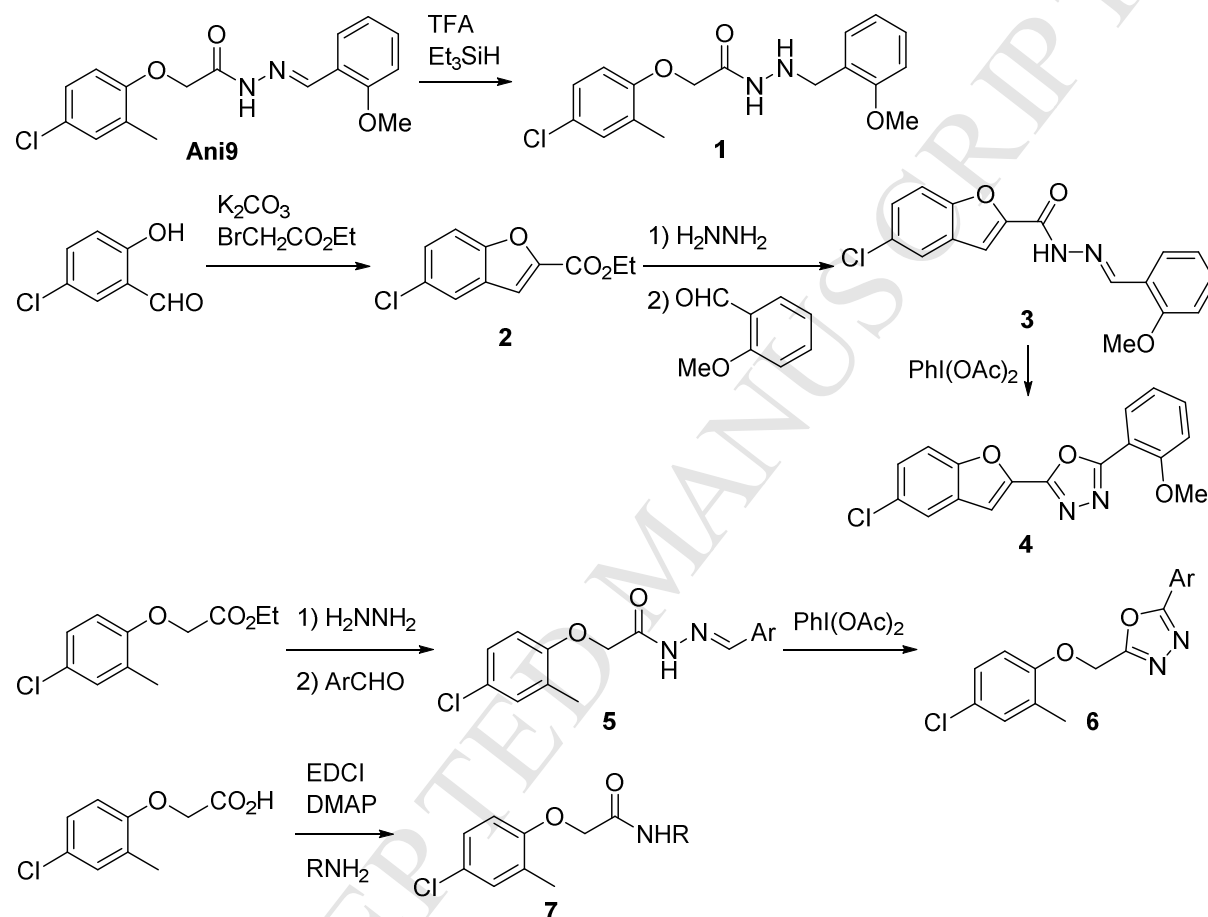


Results and discussion

Our synthetic plans for Ani9 derivatization is outlined in Scheme 2. Reduction of the hydrazone unit in Ani9 with NaBH_4 afforded acylhydrazine **1**. As conformational restriction of initial hit compounds via additional ring introduction may result in more potent biological activities, benzofuran analogue **3** was synthesized (Scheme 2). To evaluate the substituent effect of the phenyl ring in Ani9, acylhydrazone derivatives **5** were prepared. Acylhydrazide derived from ethyl 4-chloro-2-methylphenoxyacetate was allowed to react with various (hetero)arylaldehydes to afford **5**. The corresponding oxadiazoles **6** were obtained by oxidative ring closure of acylhydrazones **5** to see if biological activity could be retained with

oxadiazole unit. Furthermore, derivatives **7** having an amide instead of an acylhydrazone were synthesized by EDC coupling of the commercially available 4-chloro-2-methylphenoxyacetic acid with several amines.

Scheme 2. Syntheses of Ani9 Derivatives 1, 3-7



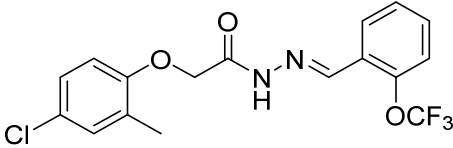
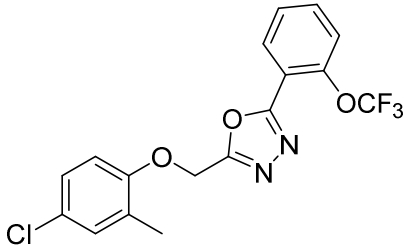
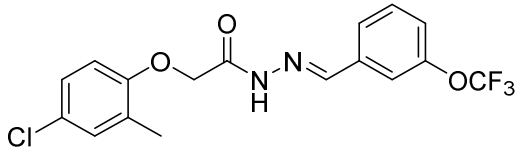
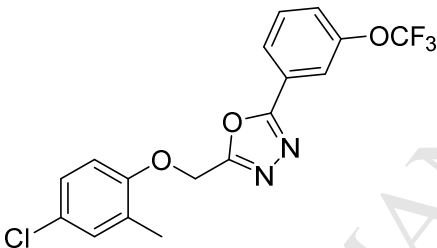
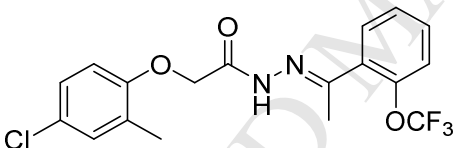
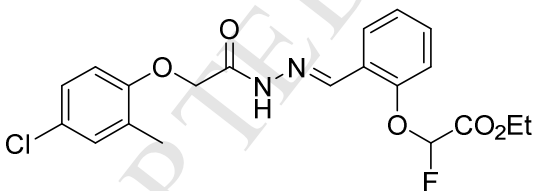
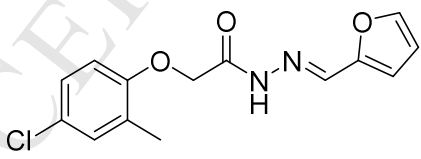
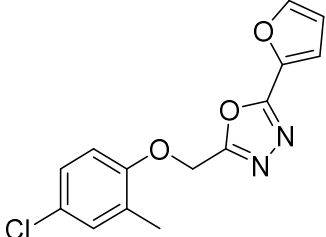
ANO1 and ANO2 inhibitory activities of the compounds were measured using YFP fluorescence quenching assay in FRT-ANO1 and -ANO2 cells (Figure 2). Hydrazone moiety of Ani9 seemed to be crucial as the corresponding hydrazine **1** exhibited the decreased activity. A conformationally restricted benzofuran analogue **3** lost ANO1 inhibitory activity. Overall, either oxadiazole (**6a-k**) or amide derivatives (**7a-f**) displayed decreased ANO1 inhibition compared with acylhydrazones (**5**). With respect to the substituent effects of the

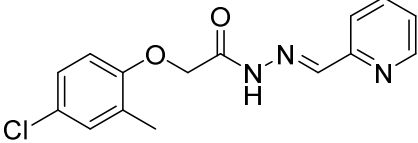
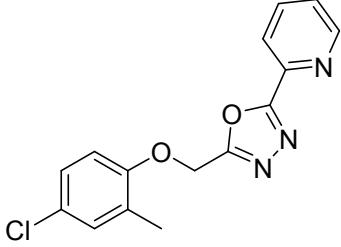
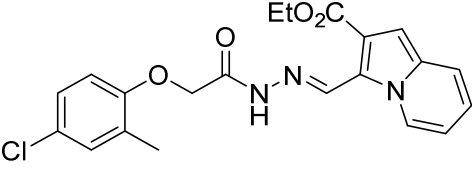
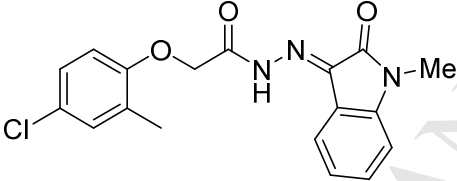
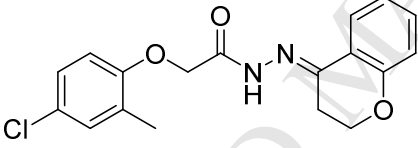
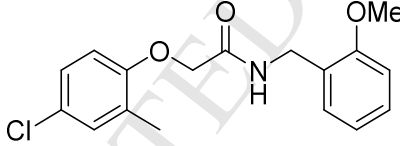
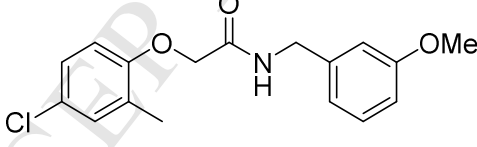
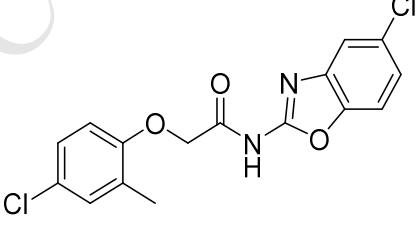
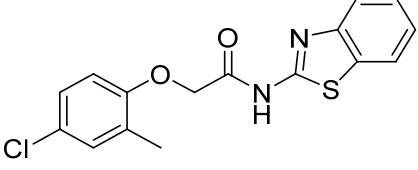
phenyl ring, substitution at the meta-position did not increase the activity. Interestingly, electron-withdrawing groups such as fluorine and trifluoromethyl at the ortho-position helped to inhibit ANO1 although the activities are less than that of Ani9. Finally, acylhydrazone (**5f**) bearing a trifluoromethoxy group at the ortho-position showed more potent ANO1 inhibitory activity than Ani9 while **5g** with a trifluoromethoxy group at the meta-position did not inhibit ANO1, indicating the importance of the orientation of this functional moiety. The corresponding ketone analogue (**5h**) displayed rather weaker activity than **5f**.

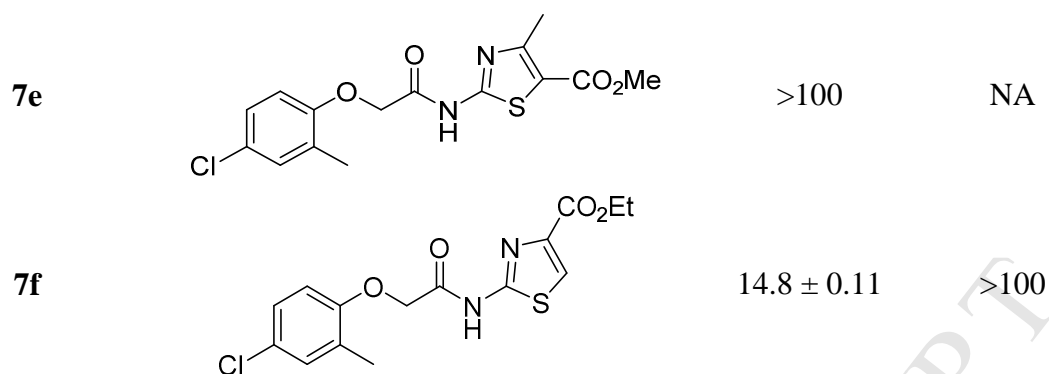
Figure 2. ANO1 and ANO2 inhibition by Ani9 analogues^a

Compound	Structure	IC ₅₀ (μM) of ANO1	IC ₅₀ (μM) of ANO2
Ani9		0.097 ± 0.01	>100
1		10.7 ± 0.14	>100
3		>100	>100
4		>100	>100
6a		19.4 ± 0.01	12.4 ± 0.05

5b		>100	NA ^b
6b		>100	>100
5c		0.89 ± 0.02	NA
6c		21.2 ± 0.17	>100
5d		>100	NA
6d		>100	>100
5e		0.21 ± 0.04	NA
6e		>100	>100

5f		0.021 ± 0.005	NA
6f		>100	NA
5g		>100	NA
6g		>100	NA
5h		0.3 ± 0.02	>100
5i		15.7 ± 0.01	59.4 ± 0.45
5j		25.7 ± 0.01	NA
6j		63.8 ± 0.02	>100

5k		31.3 ± 0.57	>100
6k		>100	NA
5l		>100	>100
5m		>100	NA
5n		>100	NA
7a		20.6 ± 0.02	13.1 ± 0.07
7b		53.7 ± 0.05	>100
7c		14.2 ± 0.07	NA
7d		>100	>100



^a IC_{50} values were determined using YFP fluorescence quenching assay in FRT cells expressing ANO1 and ANO2 (mean \pm S.E., $n = 3$). ^b NA when the inhibition rate is less than 20%.

With these results in hand, more analogues based on **5f** were prepared, which contain methyl, dimethyl, and difluoro groups at the α position of the carbonyl to see the substituent effects (Scheme 3). *O*-alkylation of 4-chloro-2-methylphenol with three different α -bromoesters followed by sequential reactions with hydrazine and 2-trifluoromethoxybenzaldehyde furnished **8a-c**, respectively. Unfortunately, these substituents did not lead to increased activity (Figure 3).

Scheme 3. Syntheses of Ani9 Derivatives **8a-c**

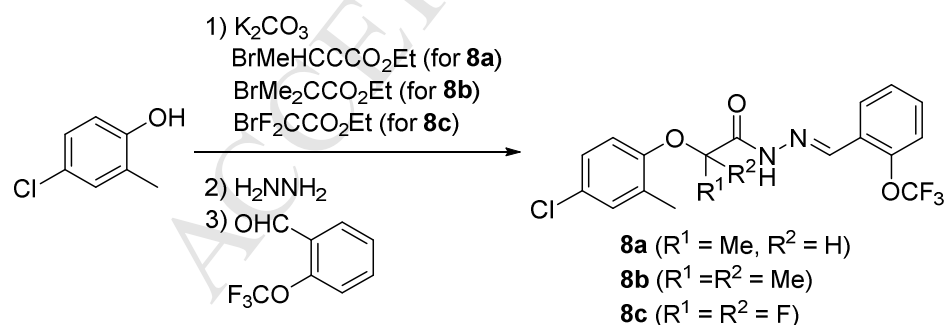
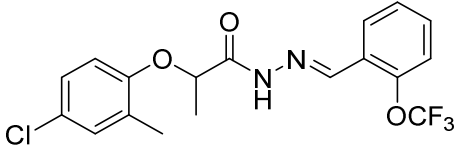
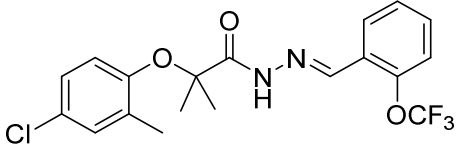
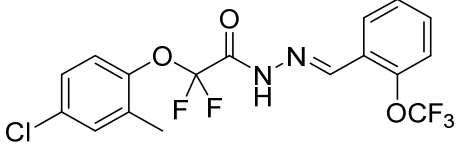


Figure 3. ANO1 and ANO2 inhibition by Ani9 analogues 8a-c^a

Compound	Structure	IC ₅₀ (μM) of ANO1	IC ₅₀ (μM) of ANO2
8a		>100	NA ^b
8b		NA	>100
8c		>100	>100

^a IC₅₀ values were determined using YFP fluorescence quenching assay in FRT cells expressing ANO1 and ANO2 (mean ± S.E., n = 3). ^b NA when the inhibition rate is less than 20%.

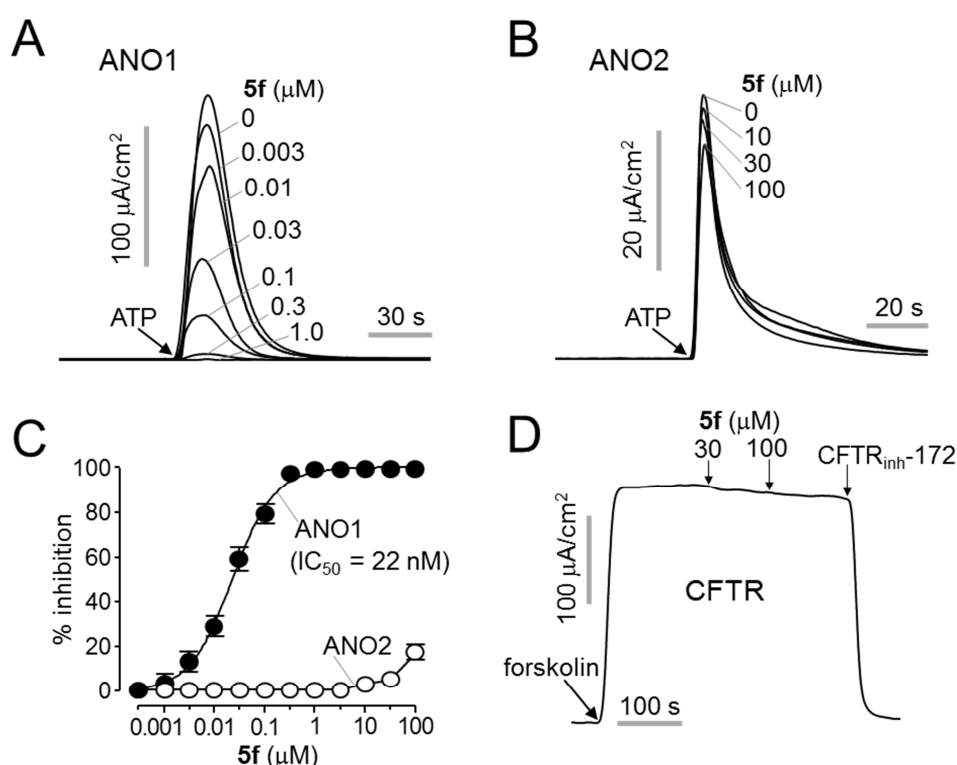
Taken together, the SAR studies led to a series of new Ani9 ((*E*)-2-(4-chloro-2-methylphenoxy)-*N'*-(2-methoxybenzylidene)acetohydrazide) derivatives as ANO1 inhibitors, and **5f** was the most potent and selective compound.

Electrophysiological studies on inhibitory effect of **5f** on chloride channels

We further determined the inhibitory effect of **5f** on ANO1, ANO2 and cystic fibrosis transmembrane conductance regulator (CFTR) using Ussing chamber study. As shown in Figure 4A and 4B, apical membrane current measurement in FRT cells expressing ANO1 and ANO2 revealed that **5f** potently inhibited ATP-induced ANO1 chloride current in a dose dependent manner with an IC₅₀ value of 22 nM (Figure 4C), but ANO2 was very poorly inhibited by **5f**. Only 17.1 ± 3.5% of ANO2 chloride current was blocked by 100 μM of **5f**. To investigate the effect of **5f** on CFTR, a cAMP-regulated apical chloride channel, CFTR

was activated by forskolin and inhibited with CFTR_{inh}-172, a selective CFTR inhibitor (Figure 4D). CFTR chloride current was not significantly altered by high concentrations (30 and 100 μM) of **5f**. These results revealed that **5f** is at least 1,000-fold more selective for ANO1 than for ANO2 and CFTR.

Figure 4. Selective inhibition of ANO1 over ANO2 by 5f

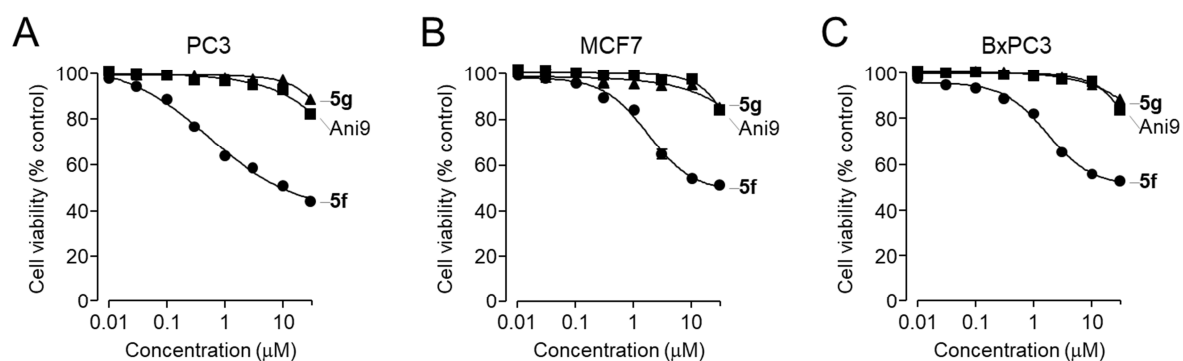


A-B) Representative apical membrane current measurement in FRT cells expressing ANO1 and ANO2. The indicated concentrations of **5f** were applied 20 minutes before ANO1 and ANO2 activation by 100 μM ATP. C) Summary of dose responses (mean \pm S.E., $n = 3-6$). D) Apical membrane current measured in FRT cells expressing human WT-CFTR cells. CFTR was activated by 20 μM forskolin and indicated concentrations of **5f** were applied. CFTR was completely inhibited by 10 μM CFTR_{inh}-172.

Effect of 5f on cell viability in PC3, MCF7 and BxPC3 cells expressing high levels of ANO1

Downregulation of ANO1 significantly reduces cell proliferation and migration in prostate, breast and pancreatic cancer cell lines expressing high levels of ANO1 (PC3, MCF7 and BxPC3, respectively) [11, 18, 19]. To investigate the effect of ANO1 inhibitors on proliferation of PC3, MCF7 and BxPC3 cells, the cells were treated with Ani9, **5f** or **5g** (a nonfunctional analogue of **5f**) for 48 hours and cell viability was estimated with MTS assay.

Figure 5. Effect of 5f, 5g and Ani9 on cell proliferation in PC3, MCF7 and BxPC3 cells



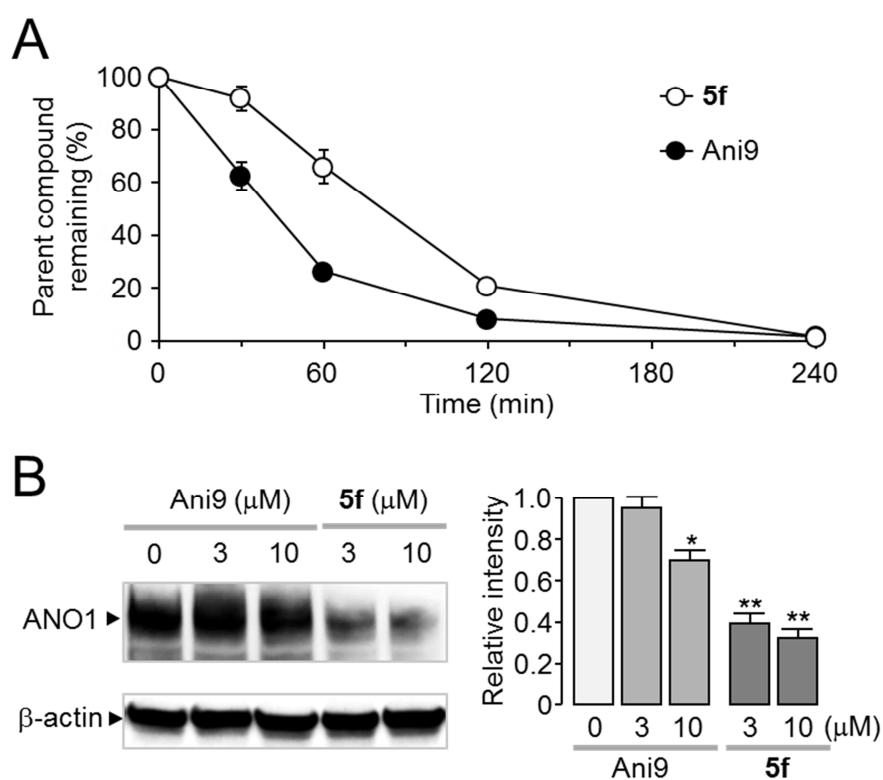
A-C) PC3, MCF7 and BxPC3 cells expressing high levels of ANO1 were treated with Ani9, **5f** and **5g** at the indicated concentration for 48 hours. Cell viability was determined by MTS assay (mean \pm S.E., n = 3).

As shown in Figure 5, high concentrations of Ani9 did not strongly inhibit the cell viability in PC3, MCF7 and BxPC3 cells. However, **5f** strongly inhibited cell viability of PC3, MCF7 and BxPC3 cells in a dose dependent manner, and the nonfunctional compound **5g** showed only small decrease in cell viability at high concentration as expected. In this experiment, **5f** much more potently inhibited the viability of prostate, breast and pancreatic cancer cells compared with Ani9, but electrophysiological studies showed that IC₅₀ values of Ani9 and **5f** are 77 and 22 nM, respectively [31].

To investigate the low activity of Ani9 on the inhibition of cell viability, we observed plasma

stability of Ani9 and **5f** and the effect of these compounds on the protein levels of ANO1 in PC3 cells expressing high levels of ANO1. As shown in Figure 6A, Ani9 showed low plasma stability but **5f** displayed longer stability in rat plasma compared to Ani9. The half-life of Ani9 and **5f** in rat plasma was 32 and 104 min, respectively. Of interest, **5f** strongly decreased protein levels of ANO1 at 3 and 10 μM , but Ani9 weakly reduced the protein levels of ANO1 only at 10 μM (Figure 6B). These results showed **5f** is a more stable, potent and selective inhibitor of ANO1 compared with Ani9.

Figure 6. Plasma stability of Ani9 and 5f, and effect of the compounds on protein levels of ANO1 in PC3 cells



A) Stability profiles of Ani9 and **5f** in rat plasma. Ani9 (5 μM) and **5f** (5 μM) were incubated in rat plasma at 37 $^{\circ}\text{C}$ for different incubation time of 0, 30, 60, 120 and 240 min. (mean \pm S.E.,

n = 3). B) Western blot analysis of ANO1 in PC3 cells expressing high levels of ANO1. Cells were incubated with indicated concentration of Ani9 and **5f** for 24 hours. (right) Summary of band-intensity. The ANO1 band intensity was normalized to β -actin (mean \pm S.E., n = 3). *P < 0.05 **P < 0.01, ***P < 0.001.

Conclusion

We have evaluated the inhibitory effect of a series of Ani9 derivatives against ANO1. The SAR analysis led to the identification of new potent ANO1 inhibitors including **5f** (with an IC₅₀ value of 22 nM). The selectivity analyses revealed that **5f** is highly selective for ANO1, showing >1,000-fold selectivity over ANO2. These results show that **5f** is currently the most potent and selective ANO1 inhibitor. In vitro studies showed that **5f** potently inhibited the viability of PC3, MCF7 and BxPC3 cells in a dose-dependent manner. In addition, **5f** showed >3 times longer plasma stability and strong reduction of ANO1 protein levels compared to Ani9. This study can be helpful in further efforts to identify potent and selective ANO1 inhibitors as a pharmacological tool in studies on ANO1, as well as a promising drug candidate for treating ANO1-related diseases.

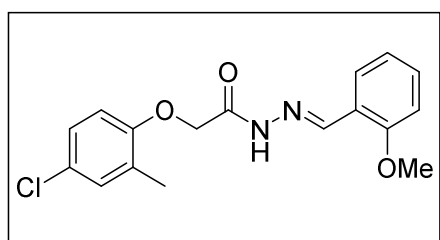
Experimental Section

General Methods

Unless specified, all reagents and starting materials were purchased from commercial sources and used as received without purification. “Concentrated” refers to the removal of volatile solvents via distillation using a rotary evaporator. “Dried” refers to pouring onto, or passing through, anhydrous magnesium sulfate followed by filtration. Flash chromatography was performed using silica gel (230–400 mesh) with hexanes, ethyl acetate, and dichloromethane as the eluent. All reactions were monitored by thin-layer chromatography on 0.25 mm silica plates (F-254) visualized with UV light. Melting points were measured using a capillary

melting point apparatus. ^1H and ^{13}C NMR spectra were recorded on a 400 MHz NMR spectrometer and were described as chemical shifts, multiplicity (s, singlet; d, doublet; t, triplet; q, quartet; m, multiplet), coupling constant in hertz (Hz), and number of protons. HRMS were measured with an electrospray ionization (ESI) and Q-TOF mass analyzer.

Synthesis of Ani9: A mixture of 2-(4-chloro-2-methylphenoxy)acetohydrazide (100 mg, 0.47 mmol) and 2-methoxybenzaldehyde (76 mg, 1.2 equiv) in EtOH (2.5 mL) was stirred at 80 °C for 16 h. The precipitated product was collected by filtration and dried to give Ani9 as a white solid.

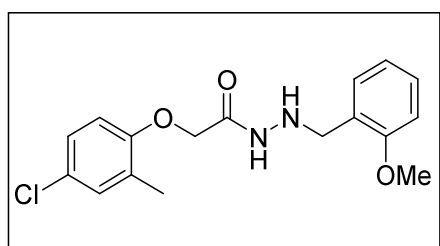


(E)-2-(4-Chloro-2-methylphenoxy)-N'-(2-methoxybenzylidene)acetohydrazide (Ani9). White

solid, mp: 160.8-162.9 °C; ^1H NMR (400 MHz, DMSO- d_6) δ 11.57 (s, 1H, isomer a), 11.56 (s, 1H, isomer b), 8.62 (s, 1H, isomer b), 8.34 (s, 1H, isomer a), 7.83 (d, $J = 7.6$ Hz, 1H, isomer a), 7.80 (d, $J = 7.6$ Hz, 1H, isomer b), 7.44-7.37 (m, 1H, isomer a, b), 7.26-7.13 (m, 1H, isomer a, b), 7.09 (d, $J = 8.4$ Hz, 1H, isomer a, b), 7.03-6.96 (m, 1H, isomer a, b), 6.88 (d, $J = 8.8$ Hz, 1H, isomer b), 6.84 (d, $J = 8.8$ Hz, 1H, isomer a), 5.16 (s, 2H, isomer a), 4.66 (s, 2H, isomer b), 3.84 (s, 3H isomer a, b), 2.23 (s, 3H, isomer b), 2.20 (s, 3H, isomer a); ^{13}C NMR (100 MHz, DMSO- d_6) δ 168.8, 164.0, 157.6, 155.3, 143.3, 139.5, 131.5, 130.1, 130.1, 129.9, 128.4, 126.4, 126.3, 125.6, 123.9, 121.9, 120.7, 113.1, 111.8, 66.6, 65.3, 55.7, 15.9; HRMS (ESI-QTOF) m/z $[\text{M}+\text{H}]^+$ calcd for $\text{C}_{17}\text{H}_{18}\text{ClN}_2\text{O}_3$ 333.1000, found 333.1005.

Synthesis of 1: To a solution of Ani9 (20 mg, 0.06 mmol) in TFA (1 mL) was added Et_3SiH

(19.2 μL , 2 equiv) at 0 $^{\circ}\text{C}$. After being stirred at 0 $^{\circ}\text{C}$ for 1 h, the reaction mixture was diluted with 15% aq. HCl (1 mL) and washed with hexanes (1 mL). Then, the aqueous layer was carefully basified with KOH pellet and extracted with CH_2Cl_2 (1 mL \times 2). The organic layer was dried over MgSO_4 and concentrated under reduced pressure to give the crude residue, which was purified by silica gel column chromatography (hexanes:ethyl acetate:dichloromethane = 10:1:2) to give **1** as a white solid.



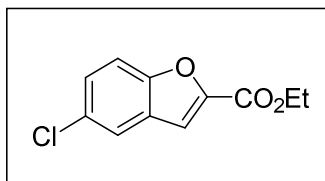
2-(4-Chloro-2-methylphenoxy)-N'-(2-

methoxybenzyl)acetohydrazide (1). White solid, mp:

98.2-100.6 $^{\circ}\text{C}$; $^1\text{H NMR}$ (400 MHz, CDCl_3) δ 7.73 (br s, 1H), 7.29 (t, $J = 7.0$ Hz, 1H), 7.18 (dd, $J = 1.2, 7.6$ Hz,

1H), 7.14-7.09 (m, 2H), 6.93-6.87 (m, 2H), 6.56 (d, $J = 8.4$ Hz, 1H), 5.04 (s, 1H), 4.50 (s, 2H), 4.04 (s, 2H), 3.86 (s, 3H), 2.11 (s, 3H); $^{13}\text{C NMR}$ (100 MHz, CDCl_3) δ 166.8, 158.1, 154.0, 131.0, 130.9, 129.5, 128.5, 126.9, 126.8, 125.1, 120.6, 112.5, 110.6, 67.5, 55.6, 51.7, 16.3; **HRMS** (ESI-QTOF) m/z $[\text{M}+\text{H}]^+$ calcd for $\text{C}_{17}\text{H}_{20}\text{ClN}_2\text{O}_3$ 335.1157, found 335.1154.

Synthesis of 2: A mixture of 5-chloro-2-hydroxybenzaldehyde (300 mg, 1.91 mmol), ethyl bromoacetate (0.25 mL, 1.2 equiv), and K_2CO_3 (795 mg, 3 equiv) in CH_3CN (6.5 mL) was stirred at 130 $^{\circ}\text{C}$ for 6 h. After being concentrated under reduced pressure, the reaction mixture was diluted with CH_2Cl_2 (5 mL) and water. The water layer was extracted with CH_2Cl_2 (5 mL) one more time. The organic layer was dried over MgSO_4 and concentrated *in vacuo* to give the crude residue, which was purified with silica gel column chromatography (hexanes:ethyl acetate:dichloromethane = 50:1:2) to afford **2** as a white solid.

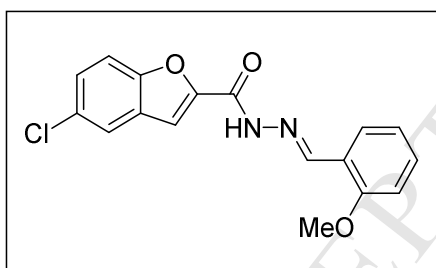


Ethyl 5-chlorobenzofuran-2-carboxylate (2). White solid, mp:

49.1-51.3 °C; $^1\text{H NMR}$ (400 MHz, CDCl_3) δ 7.63 (d, $J = 2.4$ Hz, 1H), 7.50 (d, $J = 9.2$ Hz, 1H) 7.44 (s, 1H), 7.38 (dd, $J = 2.0, 8.8$

Hz, 1H), 4.44 (q, $J = 7.2$ Hz, 2H), 1.42 (t, $J = 6.7$ Hz, 3H); $^{13}\text{C NMR}$ (100 MHz, CDCl_3) δ 159.3, 154.0, 147.1, 129.5, 128.3, 128.0, 122.3, 113.5, 113.1, 61.9, 14.4; **HRMS** (ESI-QTOF) m/z $[\text{M}+\text{H}]^+$ calcd for $\text{C}_{11}\text{H}_{10}\text{ClO}_3$ 225.0313, found 225.0315.

Synthesis of 3: A mixture of **2** (50 mg, 0.23 mmol) and hydrazine (36 μL , 5 equiv) in EtOH (1 mL) was stirred at 80 °C for 3 h. After being concentrated under reduced pressure, the crude residue (acylhydrazide) was redissolved in EtOH (1 mL) and 2-methoxybenzaldehyde (36.5 mg, 1.2 equiv) was added at rt. After being stirred at 80 °C for 16 h, the resulting precipitated product was collected by filtration and dried to give **3** as a white solid.



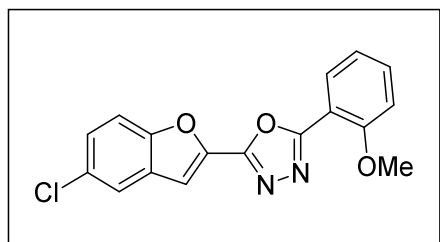
(E)-5-Chloro-*N'*-(2-methoxybenzylidene)benzofuran-2-carbohydrazide (3). White solid, mp: 193.0-196.0 °C;

$^1\text{H NMR}$ (400 MHz, $\text{DMSO}-d_6$) δ 12.22 (s, 1H), 8.87 (s, 1H), 7.93 (s, 1H), 7.88 (d, $J = 7.6$ Hz, 1H), 7.77-7.70 (m,

2H), 7.51 (dd, $J = 2.0, 8.8$ Hz, 1H), 7.44 (t, $J = 7.8$ Hz, 1H), 7.11 (d, $J = 8.4$ Hz, 1H), 7.03 (t, $J = 7.6$ Hz, 1H), 3.88 (s, 3H); $^{13}\text{C NMR}$ (100 MHz, $\text{DMSO}-d_6$) δ 157.9, 154.2, 152.9, 149.3, 144.3, 131.9, 128.6, 128.2, 127.1, 125.6, 122.3, 122.1, 120.8, 113.6, 111.9, 110.1, 55.7; **HRMS** (ESI-QTOF) m/z $[\text{M}+\text{H}]^+$ calcd for $\text{C}_{17}\text{H}_{14}\text{ClN}_2\text{O}_3$ 329.0687, found 329.0688.

Synthesis of 4: To a solution of **3** (30 mg, 0.091 mmol) in CH_2Cl_2 (1 mL) was added

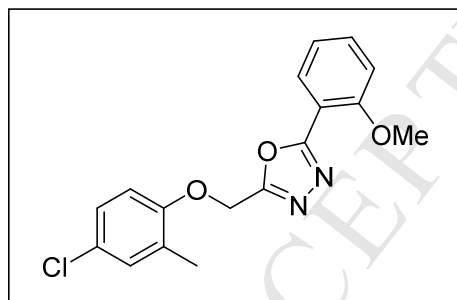
iodobenzene diacetate (32 mg, 1.1 equiv) at rt. After being stirred at rt for 6 h, the reaction mixture was concentrated *in vacuo* to furnish the crude residue, which was purified by silica gel column chromatography (hexanes:ethyl acetate:dichloromethane = 10:1:2 to 7:1:2) to give **4** as a light yellow solid.



2-(5-Chlorobenzofuran-2-yl)-5-(2-methoxyphenyl)-

1,3,4-oxadiazole (4). Light yellow solid, mp: 156.4-159.0 °C; $^1\text{H NMR}$ (400 MHz, CDCl_3) δ 8.04 (d, $J = 7.6$ Hz, 1H), 7.68 (d, $J = 1.6$ Hz, 1H), 7.60-7.49 (m, 3H),

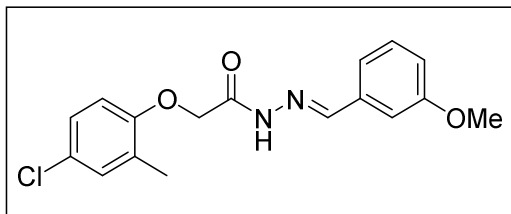
7.40 (dd, $J = 2.0, 8.8$ Hz, 1H), 7.15-7.07 (m, 2H), 4.02 (s, 3H); $^{13}\text{C NMR}$ (100 MHz, CDCl_3) δ 163.7, 158.2, 157.3, 154.1, 142.4, 133.7, 130.8, 129.8, 128.8, 127.4, 121.8, 121.0, 113.3, 112.4, 112.1, 109.3, 56.2; **HRMS** (ESI-QTOF) m/z $[\text{M}+\text{H}]^+$ calcd for $\text{C}_{17}\text{H}_{12}\text{ClN}_2\text{O}_3$ 327.0531, found 327.0532.



2-((4-Chloro-2-methylphenoxy)methyl)-5-(2-methoxyphenyl)-1,3,4-oxadiazole (6a). White solid, mp: 104.8-105.9 °C; $^1\text{H NMR}$ (400 MHz, CDCl_3) δ 7.93 (d, $J = 8.0$ Hz, 1H), 7.52 (t, $J = 8.0$ Hz, 1H), 7.16-7.04 (m, 4H), 6.95 (d, $J = 8.8$ Hz, 1H), 5.231 (s, 2H),

3.95 (s, 3H), 2.23 (s, 3H); $^{13}\text{C NMR}$ (100 MHz, CDCl_3) δ 164.7, 162.0, 158.1, 154.6, 133.6, 131.0, 129.5, 126.8, 126.7, 120.9, 113.2, 112.7, 112.1, 60.7, 56.1, 16.3; **HRMS** (ESI-QTOF) m/z $[\text{M}+\text{Na}]^+$ calcd for $\text{C}_{17}\text{H}_{15}\text{ClN}_2\text{NaO}_3$ 355.0820, found 355.0822.

Compounds **5b-5n** and **6b-6k** were prepared by following the similar procedures as those for the syntheses of **3** and **4**.

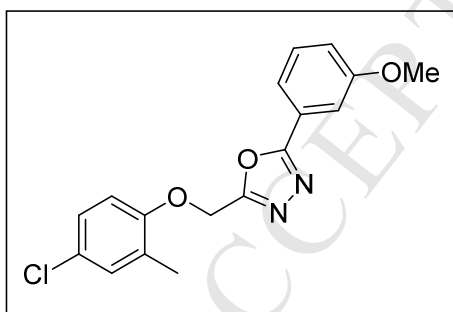


(E)-2-(4-Chloro-2-methylphenoxy)-N'-(3-methoxybenzylidene)acetohydrazide (5b). White

solid, mp: 188.2-190.5 °C; $^1\text{H NMR}$ (400 MHz,

DMSO- d_6) δ 11.64 (s, 1H, isomer a), 11.55 (s, 1H,

isomer b), 8.26 (s, 1H, isomer b), 7.97 (s, 1H, isomer a), 7.45-7.1 (m, 4H, isomer a, b), 7.0 (s, 1H, isomer a, b), 6.95-6.75 (m, 1H, isomer a, b), 5.18 (s, 2H, isomer a) 4.69 (s, 2H, isomer b), 3.78 (s, 3H, isomer a, b), 2.30-2.13 (m, 3H, isomer a, b); $^{13}\text{C NMR}$ (100 MHz, DMSO- d_6) δ 169.0, 164.2, 159.5, 155.3, 154.9, 147.8, 143.7, 135.5, 135.4, 130.1, 130.0, 129.9, 128.8, 128.4, 126.4, 126.3, 124.5, 123.9, 120.1, 119.6, 116.4, 115.9, 113.2, 113.0, 111.5, 111.3, 66.9, 65.3, 55.2, 15.9; **HRMS** (ESI-QTOF) m/z $[\text{M}+\text{H}]^+$ calcd for $\text{C}_{17}\text{H}_{18}\text{ClN}_2\text{O}_3$ 333.1000, found 333.1003.



2-((4-Chloro-2-methylphenoxy)methyl)-5-(3-

methoxyphenyl)-1,3,4-oxadiazole (6b). Light yellow

solid, mp: 86.0-86.1 °C; $^1\text{H NMR}$ (400 MHz, CDCl_3) δ

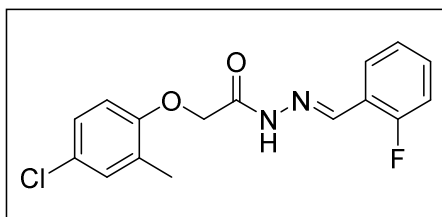
7.64 (d, $J = 7.6$ Hz, 1H), 7.59 (s, 1H) 7.42 (t, $J = 8.0$ Hz,

1H), 7.17-7.07 (m, 3H), 6.94 (d, $J = 9.2$ Hz, 1H), 5.31

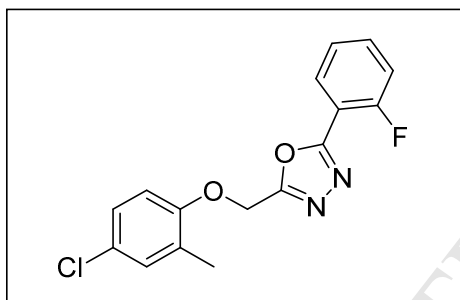
(s, 2H), 3.88 (s, 3H), 2.24 (s, 3H); $^{13}\text{C NMR}$ (100 MHz, CDCl_3) δ 165.9, 162.3, 160.1, 154.5,

131, 130.4, 129.5, 126.9, 126.7, 124.6, 119.6, 118.7, 113.1, 111.8, 60.6, 55.7, 16.2; **HRMS**

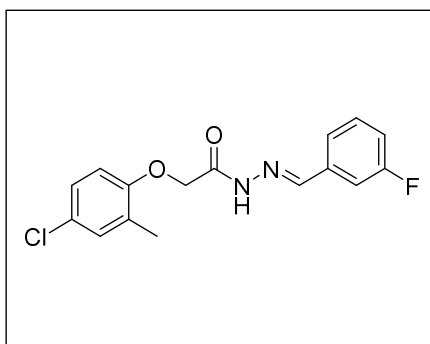
(ESI-QTOF) m/z $[\text{M}+\text{H}]^+$ calcd for $\text{C}_{17}\text{H}_{16}\text{ClN}_2\text{O}_3$ 331.0844, found 331.0845.



(E)-2-(4-Chloro-2-methylphenoxy)-N'-(2-fluorobenzylidene)acetohydrazide (5c). White solid, mp: 177.3-178.7 °C; $^1\text{H NMR}$ (400 MHz, $\text{DMSO-}d_6$) δ 11.8-11.63 (m, 1H, isomer a, b), 8.53 (s, 1H, isomer b), 8.21 (s, 1H, isomer a), 7.93 (s, 1H, isomer a, b), 7.6-7.05 (m, 5H, isomer a, b), 6.87 (s, 1H, isomer a, b), 5.19 (s, 2H, isomer a), 4.70 (s, 2H, isomer b), 2.21 (s, 3H, isomer a, b); $^{13}\text{C NMR}$ (100 MHz, $\text{DMSO-}d_6$) δ 169.0, 164.3, 161.9, 159.4, 155.2, 154.9, 136.6, 132.0, 131.9, 129.9, 128.4, 126.5, 126.4, 126.3, 124.9, 123.0, 121.6, 16.1, 115.9, 113.2, 113.1, 67.0, 65.3, 15.9; **HRMS** (ESI-QTOF) m/z $[\text{M}+\text{H}]^+$ calcd for $\text{C}_{16}\text{H}_{15}\text{ClFN}_2\text{O}_2$ 321.0801, found 321.0799.

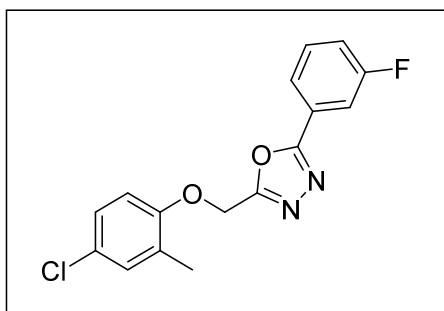


2-((4-Chloro-2-methylphenoxy)methyl)-5-(2-fluorophenyl)-1,3,4-oxadiazole (6c). White solid, mp: 96.8-98.7 °C; $^1\text{H NMR}$ (400 MHz, CDCl_3) δ 8.08 (t, $J = 7.6$ Hz, 1H), 7.60-7.53 (m, 1H), 7.31 (t, $J = 7.6$ Hz, 1H), 7.26 (t, $J = 9.2$ Hz, 1H), 7.16-7.11 (m, 2H), 6.94 (d, $J = 9.2$ Hz, 1H), 5.34 (s, 2H), 2.24 (s, 3H); $^{13}\text{C NMR}$ (100 MHz, CDCl_3) 162.7, 161.5, 158.9, 154.5, 134.1, 134.0, 131.1, 130.0, 129.99, 129.6, 127.0, 126.7, 124.9, 124.86, 117.3, 117.1, 113.1, 60.5, 16.2; **HRMS** (ESI-QTOF) m/z $[\text{M}+\text{H}]^+$ calcd for $\text{C}_{16}\text{H}_{13}\text{ClFN}_2\text{O}_2$ 319.0644, found 319.0641.



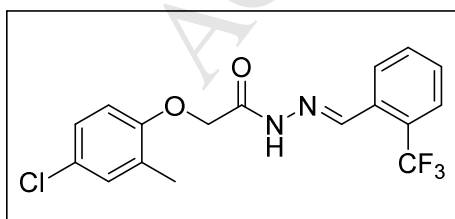
(E)-2-(4-Chloro-2-methylphenoxy)-N'-(3-fluorobenzylidene)acetohydrazide (5d). White solid,

mp: 200.3-201.8 °C; $^1\text{H NMR}$ (400 MHz, $\text{DMSO-}d_6$) δ 11.7 (s, 1H, isomer a, b), 8.29 (s, 1H, isomer b) 8.0 (s, 1H, isomer a), 7.61-7.43 (m, 3H, isomer a, b), 7.32-7.12 (m, 3H, isomer a, b), 6.91-6.85 (m, 1H, isomer a, b) 5.20 (s, 2H, isomer a), 4.70 (s, 2H, isomer b), 2.23 (s, 3H, isomer b), 2.2 (s, 3H, isomer a); $^{13}\text{C NMR}$ (100 MHz, $\text{DMSO-}d_6$) δ 169.1, 164.3, 163.6, 161.2, 155.3, 154.9, 142.4, 136.6, 130.9, 130.8, 130.1, 129.9, 128.4, 126.4, 126.3, 123.9, 123.6, 116.8, 113.1, 112.9, 112.7, 66.9, 65.3, 15.9; **HRMS** (ESI-QTOF) m/z $[\text{M}+\text{H}]^+$ calcd for $\text{C}_{16}\text{H}_{15}\text{ClFN}_2\text{O}_2$ 321.0801, found 321.0806.



2-((4-Chloro-2-methylphenoxy)methyl)-5-(3-fluorophenyl)-1,3,4-oxadiazole (6d). White solid, mp: 85.2-87.8 °C; $^1\text{H NMR}$ (400 MHz, CDCl_3) δ 7.87 (d, J = 8.0 Hz, 1H), 7.77 (d, J = 9.2 Hz, 1H), 7.55-7.47 (m, 1H), 7.3-7.23 (m, 1H), 7.17-7.12 (m, 2H), 6.93 (d, J =

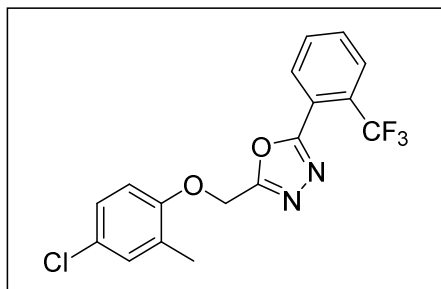
8.4 Hz, 1H), 5.32 (s, 2H), 2.24 (s, 3H); $^{13}\text{C NMR}$ (100 MHz, CDCl_3) δ 165.0, 164.96, 164.2, 162.6, 161.7, 154.5, 131.2, 131.1, 131.1, 129.5, 127.0, 126.7, 125.5, 125.4, 123.0, 122.98, 119.5, 119.3, 114.4, 114.2, 113.0, 60.5, 16.2; **HRMS** (ESI-QTOF) m/z $[\text{M}+\text{H}]^+$ calcd for $\text{C}_{16}\text{H}_{13}\text{ClFN}_2\text{O}_2$ 319.0644, found 319.0643.



(E)-2-(4-Chloro-2-methylphenoxy)-N'-(2-(trifluoromethyl)benzylidene)acetohydrazide (5e).

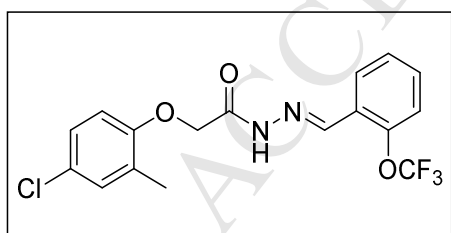
White solid, mp: 158.2-160.0 °C; $^1\text{H NMR}$ (400 MHz, $\text{DMSO-}d_6$) δ 11.95 (s, 1H, isomer b), 11.87 (s, 1H, isomer a), 8.66 (s, 1H, isomer b), 8.36 (s, 1H, isomer a), 8.22 (d, J = 8 Hz, 1H, isomer a),

8.17 (d, $J = 8$ Hz, 1H, isomer b), 7.83-7.7 (m, 3H, isomer a), 7.67-7.58 (m, 3H, isomer b), 7.27-7.12 (m, 3H, isomer a), 6.93-6.86 (m, 3H, isomer b), 5.23 (s, 2H, isomer a), 4.72 (s, 2H, isomer b), 2.24 (s, 3H, isomer b), 2.21 (s, 3H, isomer a); ^{13}C NMR (100 MHz, DMSO- d_6) δ 169.2, 164.6, 155.2, 155.0, 139.0, 132.8, 131.8, 130.1, 130.0, 129.9, 128.4, 127.1, 126.9, 126.4, 126.2, 125.9, 124.0, 113.3, 113.1, 67.0, 65.3, 15.9; HRMS (ESI-QTOF) m/z $[\text{M}+\text{H}]^+$ calcd for $\text{C}_{17}\text{H}_{15}\text{ClF}_3\text{N}_2\text{O}_2$ 371.0769, found 371.0765.



2-((4-Chloro-2-methylphenoxy)methyl)-5-(2-(trifluoromethyl)phenyl)-1,3,4-oxadiazole (6e). White solid, mp: 70.8-72.0 °C; ^1H NMR (400 MHz, CDCl_3) δ 8.09-8.05 (m, 1H), 7.89-7.85 (m, 1H), 7.74-7.70 (m, 2H), 7.17-7.11 (m, 2H), 6.91 (d, $J = 8.4$ Hz, 1H), 5.34 (s, 2H),

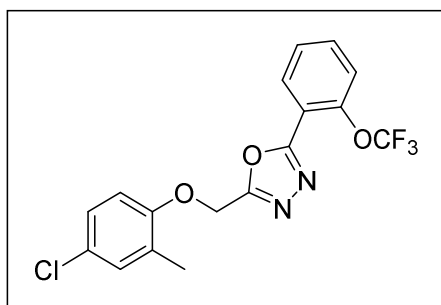
2.23 (s, 3H); ^{13}C NMR (100 MHz, CDCl_3) δ 164.4, 163.5, 154.4, 132.4, 132.4, 132.1, 132.1, 132.1, 131.1, 129.6, 126.7, 112.8, 60.4, 16.1; HRMS (ESI-QTOF) m/z $[\text{M}+\text{H}]^+$ calcd for $\text{C}_{17}\text{H}_{13}\text{ClF}_3\text{N}_2\text{O}_2$ 369.0612, found 369.0613.



(E)-2-(4-Chloro-2-methylphenoxy)-N'-(2-(trifluoromethoxy)benzylidene)acetohydrazide (5f).

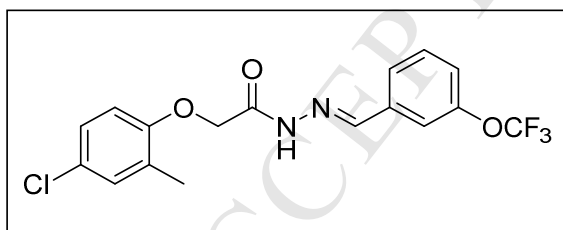
White solid, mp: 157.2-158.0 °C; ^1H NMR (400 MHz, DMSO- d_6) δ 11.83 (s, 1H, isomer b), 11.76 (s, 1H, isomer a), 8.57 (s, 1H, isomer b), 8.27 (s, 1H, isomer a), 8.06 (d, $J = 7.6$ Hz, 1H, isomer a), 8.02 (d, $J = 8.0$ Hz, 1H, isomer b), 7.62-6.54 (m, 3H, isomer b), 7.52-7.43 (m, 3H, isomer a), 7.28-7.12 (m, 3H, isomer a), 6.92-6.84 (m, 3H, isomer b), 5.2 (s, 2H, isomer a), 4.71 (s, 2H,

isomer b), 2.24 (s, 3H, isomer b), 2.21 (s, 3H, isomer a); ^{13}C NMR (100 MHz, DMSO- d_6) δ 169.0, 155.2, 140.8, 137.2, 131.6, 130.1, 129.9, 128.4, 128.1, 128.0, 127.0, 126.9, 126.6, 126.4, 126.2, 124.0, 121.8, 113.1, 67.0, 65.3, 15.9; HRMS (ESI-QTOF) m/z $[\text{M}+\text{H}]^+$ calcd for $\text{C}_{17}\text{H}_{15}\text{ClF}_3\text{N}_2\text{O}_3$ 387.0718, found 387.0719.



2-((4-Chloro-2-methylphenoxy)methyl)-5-(2-(trifluoromethoxy)phenyl)-1,3,4-oxadiazole (6f). Light yellow solid, mp: 85.6-86.6 °C; ^1H NMR (400 MHz, CDCl_3) δ 8.18 (d, $J = 7.2$ Hz, 1H), 7.62 (t, $J = 7.2$ Hz, 1H), 7.52-7.41 (m, 2H), 7.18-7.09 (m, 2H), 6.92 (d, $J =$

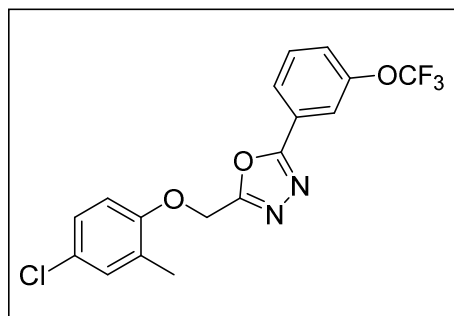
8.0 Hz, 1H), 5.34 (s, 2H), 2.23 (s, 3H); ^{13}C NMR (100 MHz, CDCl_3) δ 163.2, 163.0, 154.4, 146.6, 133.5, 131.0, 130.9, 129.5, 127.6, 126.9, 126.6, 122.5, 121.8, 119.2, 117.8, 112.8, 60.4, 16.0; HRMS (ESI-QTOF) m/z $[\text{M}+\text{H}]^+$ calcd for $\text{C}_{17}\text{H}_{13}\text{ClF}_3\text{N}_2\text{O}_3$ 385.0561, found 385.0563.



(E)-2-(4-Chloro-2-methylphenoxy)-N'-(3-(trifluoromethoxy)benzylidene)acetohydrazide (5g). White solid, mp: 176.4-179.2 °C; ^1H NMR (400 MHz, DMSO- d_6) δ 11.76 (s, 1H,

isomer a), 11.70 (s, 1H, isomer b), 8.33 (s, 1H, isomer b), 8.03 (s, 1H, isomer a), 7.76-7.65 (m, 3H, isomer a), 7.62-7.53 (m, 3H, isomer b), 7.42 (t, $J = 8.4$ Hz, 1H, isomer a, b), 7.28-7.12 (m, 3H, isomer a), 6.92-6.83 (m, 3H, isomer b), 5.20 (s, 2H, isomer a), 4.71 (s, 2H, isomer b), 2.24 (s, 3H, isomer b), 2.20 (s, 3H, isomer a); ^{13}C NMR (100 MHz, DMSO- d_6) δ 169.2, 164.4, 155.2, 154.9, 148.8, 146.1, 142.1, 136.6, 136.5, 131.0, 130.8, 130.1, 129.9, 128.7,

128.4, 126.4, 126.4, 126.2, 124.5, 123.9, 122.5, 122.1, 121.3, 118.8, 118.7, 113.2, 113.1, 67.0, 65.3, 15.9; **HRMS** (ESI-QTOF) m/z $[M+H]^+$ calcd for $C_{17}H_{15}ClF_3N_2O_3$ 387.0718, found 387.0715.

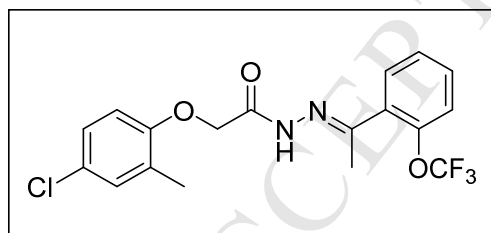


2-((4-Chloro-2-methylphenoxy)methyl)-5-(3-

(trifluoromethoxy)phenyl)-1,3,4-oxadiazole (6g).

White solid, mp: 80.3-80.8 °C; 1H NMR (400 MHz, $CDCl_3$) δ 8.02 (d, $J = 8.0$ Hz, 1H), 7.93 (s, 1H), 7.58 (t, $J = 8.0$ Hz, 1H), 7.42 (d, $J = 8.4$, 1H), 7.17-7.10 (m,

2H), 6.94 (d, $J = 8.0$ Hz, 1H), 5.33 (s, 2H), 2.24 (s, 3H); ^{13}C NMR (100 MHz, $CDCl_3$) δ 164.7, 162.7, 154.4, 149.8, 131.1, 131.0, 129.5, 127.1, 126.7, 125.5, 125.4, 124.6, 121.8, 119.7, 113.0, 60.5, 16.2; **HRMS** (ESI-QTOF) m/z $[M+H]^+$ calcd for $C_{17}H_{13}ClF_3N_2O_3$ 385.0561, found 385.0568.



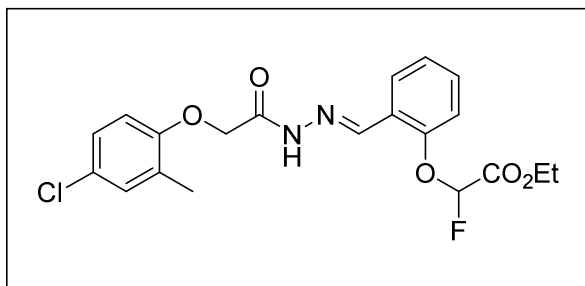
(E)-2-(4-Chloro-2-methylphenoxy)-N'-(1-(2-

(trifluoromethoxy)phenyl)ethylidene)acetohydrazide (5h).

White solid, mp: 119.2-121.0 °C; 1H NMR (400 MHz, $CDCl_3$) δ 9.56 (s, 1H, isomer a), 9.35 (s,

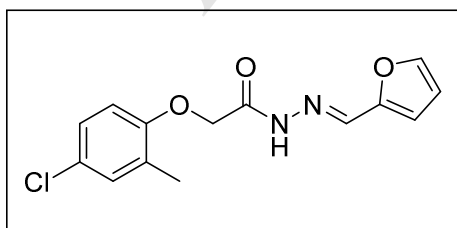
1H, isomer b), 7.67 (d, $J = 7.6$ Hz, 1H, isomer a), 7.48 (d, $J = 7.6$ Hz, 1H, isomer b), 7.52-7.4 (m, 3H, isomer b), 7.37-7.28 (m, 3H, isomer a), 7.23-7.15 (m, 2H, isomer a), 7.12 (s, 1H, isomer b), 7.05 (dd, $J = 2.0, 8.6$ Hz, 1H, isomer b), 5.09 (s, 2H, isomer b), 4.69 (s, 2H, isomer a), 2.34 (s, 3H, isomer a), 2.32-2.26 (m, 3H, isomer a, b), 2.21 (s, 3H, isomer b); ^{13}C NMR (100 MHz, $CDCl_3$) δ 170.4, 163.7, 155.1, 153.5, 152.4, 147.8, 146.9, 146.7, 131.0, 130.8,

130.8, 130.6, 130.5, 130.0, 127.1, 127.0, 127.96, 126.2, 1120.5, 112.6, 112.4, 67.4, 66.1, 16.4, 16.3, 16.2, 16.16; **HRMS** (ESI-QTOF) m/z $[M+H]^+$ calcd for $C_{18}H_{17}ClFN_2O_3$ 401.0874, found 401.0873.



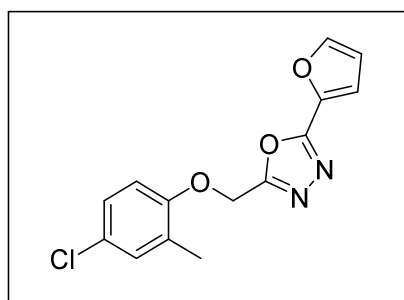
Ethyl (E)-2-((2-((2-(4-chloro-2-methylphenoxy)acetyl)hydrazono)methyl)phenoxy)-2-fluoroacetate (5i). White solid, mp: 100.3-101.5 °C; 1H NMR (400 MHz, $CDCl_3$) δ 9.50 (s, 1H, isomer a), 9.03 (s, 1H,

isomer b), 8.51 (s, 1H, isomer a), 8.20-8.15 (m, 1H, isomer a, b), 7.91 (d, $J = 7.2$ Hz, isomer b), 7.47-7.40 (m, 1H, isomer a, b), 7.25-7.12 (m, 4H for isomer a, 3H for isomer b), 7.07 (dd, $J = 8.4$ Hz, 1H, isomer b), 6.77 (d, $J = 8.4$ Hz, 1H, isomer a), 6.71 (d, $J = 8.8$ Hz, 1H, isomer b), 6.05-5.86 (m, 1H, isomer a, b), 5.13 (s, 2H, isomer b), 4.66 (s, 2H, isomer a), 4.41-4.32 (m, 2H, isomer a, b), 2.33 (s, 3H, isomer a), 2.30 (s, 3H, isomer b), 1.40-1.32 (m, 3H, isomer a, b); ^{13}C NMR (100 MHz, $CDCl_3$) δ 169.4, 164.1, 163.8, 155.1, 154.4, 153.9, 144.0, 139.5, 132.3, 132.0, 131.0, 130.7, 127.6, 127.0, 126.2, 125.0, 116.9, 116.7, 113.1, 112.7, 103.9, 103.8, 101.6, 101.56, 67.8, 66.2, 62.9, 62.8, 16.3, 16.2, 14.0, 13.99; **HRMS** (ESI-QTOF) m/z $[M+Na]^+$ calcd for $C_{20}H_{20}ClFN_2NaO_5$ 445.0937, found 445.0936.



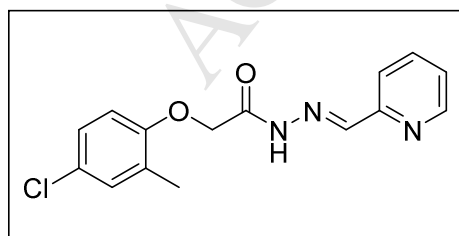
(E)-2-(4-Chloro-2-methylphenoxy)-N'-(furan-2-ylmethylene)acetohydrazide (5j). White solid, mp: 140.5-143.7 °C; 1H NMR (400 MHz, $DMSO-d_6$) δ

11.57 (s, 1H, isomer a), 11.48 (s, 1H, isomer b), 8.18 (s, 1H, isomer b), 7.89 (s, 1H, isomer a), 7.86-7.81 (m, 1H, isomer a, b), 7.27-7.11 (m, 2H, isomer a, b), 6.93-6.90 (m, 1H, isomer a, b), 6.88 (d, $J = 8.8$ Hz, 1H, isomer b), 6.8 (d, $J = 8.8$ Hz, 1H, isomer a), 6.65-6.61 (m, 1H, isomer a, b), 5.09 (s, 2H, isomer a), 4.67 (s, 2H, isomer b), 2.23 (s, 3H, isomer b), 2.20 (s, 3H, isomer a); ^{13}C NMR (100 MHz, DMSO- d_6) δ 168.6, 164.1, 155.2, 154.9, 149.1, 149.0, 145.4, 145.1, 137.7, 134.0, 130.1, 129.9, 128.8, 128.4, 126.4, 126.3, 124.6, 124.0, 114.0, 113.8, 113.2, 113.0, 112.2, 112.19, 67.0, 65.0, 15.9; HRMS (ESI-QTOF) m/z $[\text{M}+\text{H}]^+$ calcd for $\text{C}_{14}\text{H}_{14}\text{ClN}_2\text{O}_3$ 293.0687, found 293.0687.



2-((4-Chloro-2-methylphenoxy)methyl)-5-(furan-2-yl)-1,3,4-oxadiazole (6j). White solid, mp: 110.6-112.3 °C; ^1H NMR (400 MHz, CDCl_3) 7.66 (s, 1H), 7.21 (d, $J = 3.6$ Hz, 1H), 7.16-7.10 (m, 2H), 6.92 (d, $J = 8.0$ Hz, 1H), 6.62 (dd, $J = 3.2$ Hz, 1H), 5.30 (s, 2H), 2.23 (s, 3H); ^{13}C NMR (100

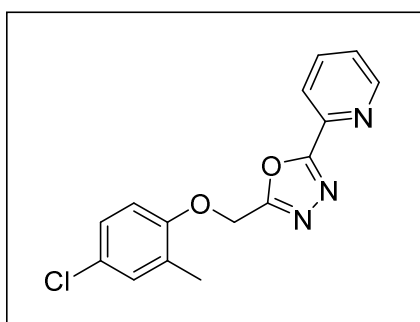
MHz, CDCl_3) δ 161.6, 158.7, 154.4, 146.2, 139.1, 131.1, 129.5, 127.0, 126.7, 115.0, 113.0, 112.4, 60.3, 16.2; HRMS (ESI-QTOF) m/z $[\text{M}+\text{H}]^+$ calcd for $\text{C}_{14}\text{H}_{12}\text{ClN}_3\text{O}_2$ 291.0531, found 291.0530.



(E)-2-(4-Chloro-2-methylphenoxy)-N'-(pyridin-2-ylmethylene)acetohydrazide (5k). White solid, mp: 179.8-180.2 °C; ^1H NMR (400 MHz, DMSO- d_6) δ 11.81 (s, 1H, isomer a, b), 8.61 (s, 1H, isomer a, b),

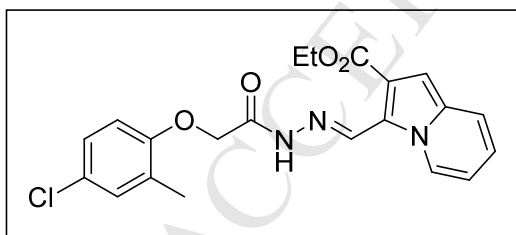
8.31 (s, 1H, isomer b), 8.04 (s, 1H, isomer a), 8.02-7.80 (m, 2H, isomer a, b), 7.41 (s, 1H,

isomer a, b), 7.28-7.10 (m, 2H, isomer a, b), 6.95-6.64 (m, 1H, isomer a, b), 5.21 (s, 2H), 4.72 (s, 2H), 2.29-2.15 (m, 3H, isomer a, b); ^{13}C NMR (100 MHz, DMSO- d_6) δ 169.1, 164.5, 155.2, 154.9, 152.8, 149.6, 149.5, 148.0, 144.3, 136.9, 136.8, 130.1, 129.9, 128.8, 128.4, 126.4, 126.3, 124.6, 124.4, 124.0, 120.0, 119.8, 113.3, 113.1, 66.9, 65.2, 15.9; HRMS (ESI-QTOF) m/z $[\text{M}+\text{H}]^+$ calcd for $\text{C}_{15}\text{H}_{15}\text{ClN}_3\text{O}_2$ 304.0847, found 304.0843.



2-((4-Chloro-2-methylphenoxy)methyl)-5-(pyridin-2-yl)-1,3,4-oxadiazole (6k). White solid, mp: 118.3-120.0 °C; ^1H NMR (400 MHz, CDCl_3) δ 8.80 (d, $J = 4.4$ Hz, 1H), 8.27 (d, $J = 8.0$ Hz, 1H), 7.95-7.87 (m, 1H), 7.50 (dd, $J = 5.2, 6.8$ Hz, 1H), 7.16-7.10 (m, 2H), 6.94 (d, $J =$

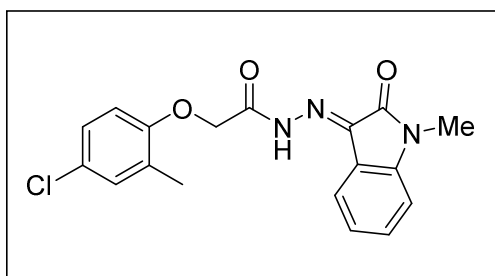
9.2 Hz, 1H), 5.35 (s, 2H), 2.23 (s, 3H); ^{13}C NMR (100 MHz, CDCl_3) δ 164.9, 163.1, 154.3, 150.4, 143.1, 137.3, 130.9, 129.4, 126.7, 126.5, 126.2, 123.4, 112.7, 60.2, 16.1; HRMS (ESI-QTOF) m/z $[\text{M}+\text{H}]^+$ calcd for $\text{C}_{15}\text{H}_{13}\text{ClN}_3\text{O}_2$ 302.0691, found 302.0690.



Ethyl (E)-3-((2-(2-(4-chloro-2-methylphenoxy)acetyl)hydrazono)methyl)indoline-2-carboxylate (5l). Yellow solid, mp: 169.0-170.2 °C; ^1H NMR (400 MHz, DMSO- d_6) δ 11.81

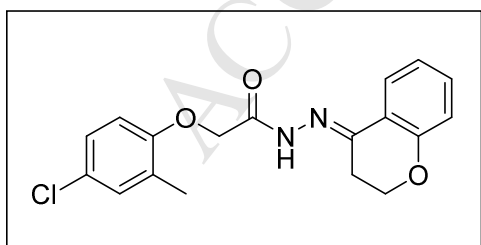
(s, 1H, isomer b), 11.74 (s, 1H, isomer b), 9.70 (d, $J = 6.8$ Hz, 1H, isomer b), 9.32 (d, $J = 6.4$ Hz, 1H, isomer a), 9.21 (s, 1H, isomer b), 9.00 (s, 1H, isomer a), 7.73 (t, $J = 8$ Hz, 1H, isomer a, b), 7.28-6.84 (m, 6H, isomer a, b), 5.24 (s, 2H, isomer a), 4.73 (s, 2H, isomer b), 4.38-4.27 (m, 2H, isomer a, b), 2.29-2.15 (m, 3H, isomer a, b) 1.41-1.28 (m, 3H, isomer a, b); ^{13}C

NMR (100 MHz, DMSO- d_6) δ 168.4, 163.8, 155.3, 155.0, 140.1, 137.1, 134.5, 134.4, 130.1, 129.9, 128.2, 127.7, 126.4, 126.3, 121.7, 121.5, 120.2, 115.0, 113.2, 113.0, 104.1, 104.0, 66.9, 65.5, 60.5, 16.0, 14.2; **HRMS** (ESI-QTOF) m/z $[M+H]^+$ calcd for $C_{21}H_{21}ClN_3O_4$ 414.1215, found 414.1218.



(E)-2-(4-Chloro-2-methylphenoxy)-N'-(1-methyl-2-oxoindolin-3-ylidene)acetohydrazide (5m). Yellow solid, mp: 209.3-210.8 °C; **1H NMR** (400 MHz, $CDCl_3$) δ 13.81 (s, 1H, isomer a), 12.63

(s, 1H, isomer b), 7.83 (d, $J = 7.6$ Hz, 2H, isomer a), 7.58 (d, $J = 7.2$ Hz, 2H, isomer b), 7.41 (t, $J = 7.6$ Hz, 1H, isomer a, b), 7.22-7.11 (m, 3H, isomer a, b), 6.88 (d, $J = 8$ Hz, 1H, isomer a, b), 6.74 (d, $J = 8.4$ Hz, 1H, isomer a, b), 5.24 (s, 2H, isomer b), 4.75 (s, 2H, isomer a), 3.27 (s, 3H, isomer a, b), 2.44 (s, 3H, isomer a), 2.31 (s, 1H, isomer b); **^{13}C NMR** (100 MHz, $CDCl_3$) δ 166.1, 161.2, 153.9, 144.1, 138.9, 132.2, 131.2, 129.4, 126.9, 126.7, 123.7, 123.6, 122.4, 121.0, 119.5, 112.1, 109.1, 67.5, 66.0, 26.0, 25.6, 16.6, 16.4; **HRMS** (ESI-QTOF) m/z $[M+H]^+$ calcd for $C_{18}H_{17}ClN_3O_3$ 358.0953, found 358.0958.

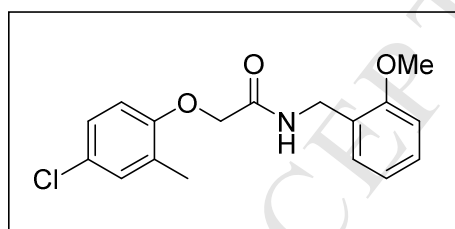


(E)-2-(4-Chloro-2-methylphenoxy)-N'-(chroman-4-ylidene)acetohydrazide (5n). White solid, mp: 215.4-217.5 °C; **1H NMR** (400 MHz, DMSO- d_6) δ 11.96 (s, 1H, isomer a), 10.62 (s, 1H, isomer b), 8.00-

7.92 (m, 1H, isomer a, b), 7.35-7.12 (m, 3H, isomer a, b), 7.03-6.95 (m, 1H, isomer a, b), 6.90 (d, $J = 7.6$ Hz, 2H, isomer, a), 6.83 (d, $J = 8.4$ Hz, 2H, isomer b), 5.23 (s, 2H, isomer a),

4.76 (s, 2H, isomer b), 4.31-4.20 (m, 2H, isomer a, b), 2.89-2.80 (m, 2H, isomer a, b), 2.22 (s, 3H, isomer a, b); ^{13}C NMR (100 MHz, DMSO- d_6) δ 169.6, 164.1, 157.1, 156.9, 155.3, 154.9, 147.9, 142.8, 131.4, 131.0, 130.1, 129.9, 128.5, 128.3, 126.4, 126.2, 124.8, 124.7, 124.3, 123.9, 121.3, 120.3, 117.5, 117.4, 113.0, 66.5, 65.6, 64.5, 25.6, 25.1, 16.0; HRMS (ESI-QTOF) m/z $[\text{M}+\text{Na}]^+$ calcd for $\text{C}_{18}\text{H}_{17}\text{ClN}_3\text{NaO}_2$ 367.0820, found 367.0824.

Synthesis of 7a: To a solution of 2-(4-chloro-2-methylphenoxy)acetic acid (53 mg, 0.26 mmol) in CH_2Cl_2 (1 mL) were added 2-methoxybenzylamine (42 μL , 1.2 equiv), EDC-HCl (78 mg, 1.5 equiv), DMAP (2 mg, 0.05 equiv), and Et_3N (76 μL , 2 equiv) at 0 $^\circ\text{C}$. After being stirred at 40 $^\circ\text{C}$ for 16 h, the reaction mixture was diluted with CH_2Cl_2 (2 mL) and washed with 15% HCl (1 mL). The aqueous layer was extracted with CH_2Cl_2 (2 mL) one more time. The organic layer was dried over MgSO_4 and concentrated under reduced pressure to give the crude residue, which was purified by silica gel column chromatography (hexanes:ethyl acetate:dichloromethane = 20:1:2 to 10:1:2) to give **7a** as a white solid.



2-(4-Chloro-2-methylphenoxy)-N-(2-

methoxybenzyl)acetamide (7a). White solid, mp:

91.6-93.5 $^\circ\text{C}$; ^1H NMR (400 MHz, CDCl_3) δ 7.31-7.24

(m, 2H), 7.20 (br s, 1H), 7.13 (s, 1H), 7.08 (d, J = 8.4

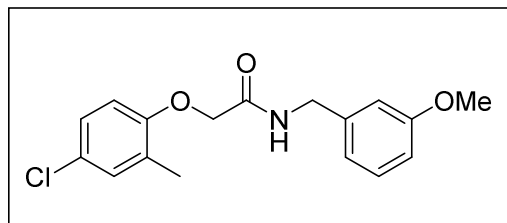
Hz, 1H), 6.93 (t, J = 7.4 Hz, 1H), 6.87 (d, J = 8.4 Hz, 1H), 6.93 (d, J = 8.8 Hz, 1H), 4.53 (d, J

= 6.0 Hz, 2H), 4.53 (s, 2H), 3.81 (s, 3H), 2.24 (s, 3H); ^{13}C NMR (100 MHz, CDCl_3) δ 167.6,

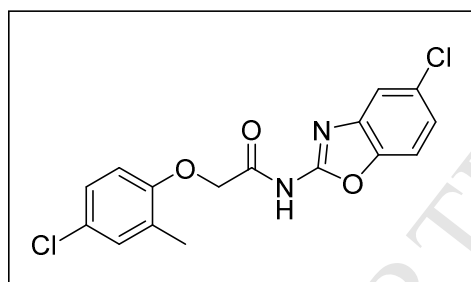
157.7, 130.8, 129.8, 129.2, 128.2, 126.9, 126.5, 125.8, 120.9, 112.5, 110.3, 67.7, 55.3, 39.4,

16.2; HRMS (ESI-QTOF) m/z $[\text{M}+\text{H}]^+$ calcd for $\text{C}_{17}\text{H}_{19}\text{ClNO}_3$ 320.1048, found 320.1045.

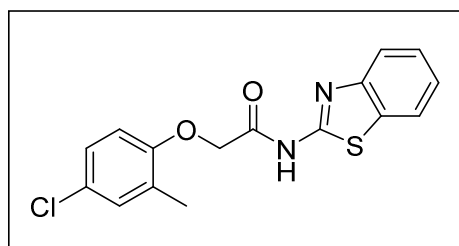
Compounds **7b-7f** were prepared by following the similar procedure as that for the synthesis of **7a**.



2-(4-Chloro-2-methylphenoxy)-N-(3-methoxybenzyl)acetamide (7b). Light yellow solid, mp: 95.8-96.5 °C; $^1\text{H NMR}$ (400 MHz, CDCl_3) δ 7.26 (t, $J = 7.8$ Hz, 1H), 7.16-7.10 (m, 2H), 6.88-6.78 (m, 4H), 6.70 (d, $J = 8.4$ Hz, 1H), 4.55-4.51 (m, 4H), 3.78 (s, 3H), 2.20 (s, 3H); $^{13}\text{C NMR}$ (100 MHz, CDCl_3) δ 168.1, 160.1, 154.1, 139.3, 131.0, 130.0, 128.5, 126.9, 119.8, 113.2, 113.2, 112.8, 68.0, 55.4, 43.1, 16.4; **HRMS** (ESI-QTOF) m/z $[\text{M}+\text{H}]^+$ calcd for $\text{C}_{17}\text{H}_{17}\text{ClNO}_3$ 320.1048, found 320.1043.

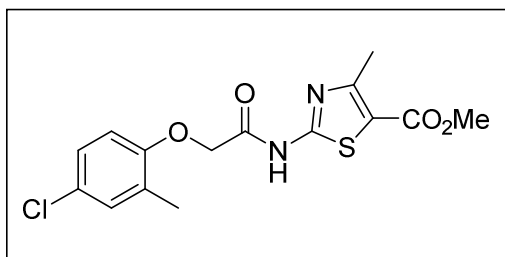


2-(4-Chloro-2-methylphenoxy)-N-(5-chlorobenzo[d]oxazol-2-yl)acetamide (7c). White solid, mp: 165.5-168.2 °C; $^1\text{H NMR}$ (400 MHz, CDCl_3) δ 9.28 (br s, 1H), 7.61 (s, 1H), 7.42 (d, $J = 8.4$ Hz, 1H), 7.27 (dd, $J = 2.0, 8.4$ Hz, 1H), 7.20 (s, 1H), 7.16 (dd, $J = 2.0, 8.4$ Hz, 1H), 6.75 (d, $J = 8.8$ Hz, 1H), 4.75 (s, 2H), 2.34 (s, 3H); $^{13}\text{C NMR}$ (100 MHz, CDCl_3) δ 165.2, 154.5, 153.5, 146.7, 131.3, 130.6, 128.7, 127.6, 127.0, 124.6, 119.2, 113.1, 111.1, 68.1, 29.7, 16.4; **HRMS** (ESI-QTOF) m/z $[\text{M}+\text{H}]^+$ calcd for $\text{C}_{16}\text{H}_{13}\text{Cl}_2\text{N}_2\text{O}_3$ 351.0298, found 351.0296.



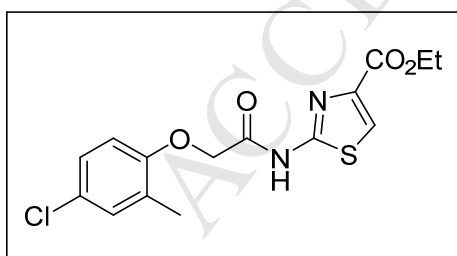
N-(Benzo[d]thiazol-2-yl)-2-(4-chloro-2-methylphenoxy)acetamide (7d). White solid, mp:

167.3-170.9 °C; $^1\text{H NMR}$ (400 MHz, CDCl_3) δ 9.70 (br s, 1H), 7.84 (d, $J = 8.0$ Hz, 1H), 7.81 (d, $J = 8.4$ Hz, 1H), 7.47 (t, $J = 7.6$ Hz, 1H), 7.35 (t, $J = 7.6$ Hz, 1H), 7.20 (s, 1H), 7.15 (d, $J = 8.8$ Hz, 1H), 6.75 (d, $J = 8.8$ Hz, 1H), 4.74 (s, 2H), 2.35 (s, 3H); $^{13}\text{C NMR}$ (100 MHz, CDCl_3) δ 166.7, 156.4, 153.7, 148.4, 131.4, 129.0, 127.1, 126.6, 124.5, 121.6, 121.5, 113.1, 67.7, 16.5; **HRMS** (ESI-QTOF) m/z $[\text{M}+\text{H}]^+$ calcd for $\text{C}_{16}\text{H}_{14}\text{ClN}_2\text{O}_2\text{S}$ 333.0459, found 333.0461.



Methyl **2-(2-(4-chloro-2-methylphenoxy)acetamido)-4-methylthiazole-5-carboxylate (7e)**. White solid, mp: 202.8-204.0 °C; $^1\text{H NMR}$ (400 MHz, CDCl_3) δ 9.55 (br s, 1H), 7.20

(s, 1H), 7.15 (dd, $J = 2.0, 8.8$ Hz, 1H), 6.73 (d, $J = 8.4$ Hz, 1H), 4.72 (s, 2H), 3.87 (s, 3H), 2.66 (s, 3H), 2.33 (s, 3H); $^{13}\text{C NMR}$ (100 MHz, CDCl_3) δ 166.4, 163.1, 157.8, 156.9, 153.6, 131.4, 128.9, 127.8, 127.1, 116.6, 113.2, 67.7, 52.1, 17.3, 16.5; **HRMS** (ESI-QTOF) m/z $[\text{M}+\text{H}]^+$ calcd for $\text{C}_{15}\text{H}_{16}\text{ClN}_2\text{O}_4\text{S}$ 355.0514, found 355.0513.

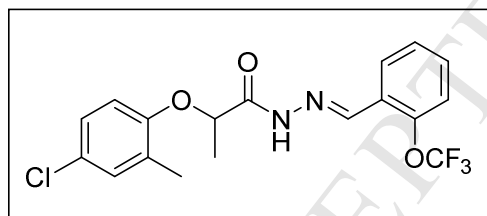


Ethyl **2-(2-(4-chloro-2-methylphenoxy)acetamido)thiazole-4-carboxylate (7f)**. White solid, mp: 154.0-155.0 °C; $^1\text{H NMR}$ (400 MHz, CDCl_3) δ 9.79 (br s, 1H), 7.90 (s, 1H), 7.19 (s,

1H), 7.13 (dd, $J = 2.4, 8.8$ Hz, 1H), 6.72 (d, $J = 8.8$ Hz, 1H), 4.73 (s, 2H), 4.41 (q, $J = 7.2$ Hz, 2H), 2.31 (s, 3H), 1.4 (t, $J = 7.0$ Hz, 3H); $^{13}\text{C NMR}$ (100 MHz, CDCl_3) δ 166.9, 161.4, 156.6, 153.7, 142.1, 131.4, 129.1, 127.7, 127.0, 122.9, 113.2, 67.8, 61.7, 16.5, 14.5; **HRMS** (ESI-

QTOF) m/z $[M+Na]^+$ calcd for $C_{15}H_{15}ClN_2NaO_4S$ 377.0333, found 377.0331.

Synthesis of 8a: To a solution of 4-chloro-2-methylphenol (100 mg, 0.7 mmol) in acetone (2.5 mL) were added methyl 2-bromopropanoate (86 μ L, 1.1 equiv) and K_2CO_3 (194 mg, 2 equiv) at rt. After being stirred at 60 °C for 16 h, the reaction mixture was concentrated under reduced pressure to afford the crude residue which was purified by silica gel chromatography (hexanes:ethyl acetate:dichloromethane = 50:1:2) to give ester (methyl 2-(4-chloro-2-methylphenoxy)propanoate) as a colorless oil. A mixture of ester (102 mg, 0.44 mmol) and hydrazine (69 μ L, 5 equiv) in EtOH (2 mL) was stirred at 80 °C for 13 h. After being concentrated under reduced pressure, the crude residue (acylhydrazide) was redissolved in EtOH (1 mL) and 2-(trifluoromethoxy)benzaldehyde (76 μ L, 1.2 equiv) was added at rt. After being stirred at 80 °C for 16 h, the resulting precipitated product was collected by filtration and dried to give **8a** as a white solid.



(E)-2-(4-Chloro-2-methylphenoxy)-N'-(2-

(trifluoromethoxy)benzylidene)propanhydrazide

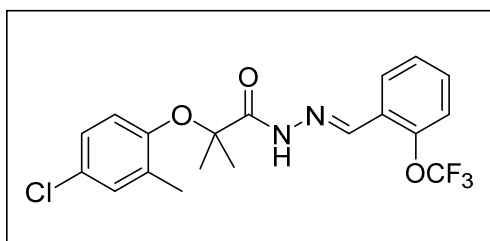
(8a). White solid, mp: 147.5-149.1 °C; 1H NMR

(400 MHz, $CDCl_3$) δ 9.55 (s, 1H, isomer a), 9.15 (s,

1H, isomer b), 8.38 (s, 1H, isomer a), 8.20 (d, $J = 7.6$ Hz, 1H, isomer a), 8.02 (s, 1H, isomer b), 7.84 (d, $J = 7.6$ Hz, 1H, isomer b), 7.49-7.41 (m, 1H, isomer a, b), 7.36-7.30 (m, 1H, isomer a, b), 7.28-7.23 (m, 1H, isomer a, b), 7.19 (s, 1H, isomer a), 7.15-7.08 (m, 1H, isomer a, b), 7.02 (dd, $J = 8.6$ Hz, 1H, isomer b), 6.78 (d, $J = 8.8$ Hz, 1H, isomer a), 6.63 (d, $J = 8.4$ Hz, 1H, isomer b), 5.55 (q, $J = 6.8$ Hz, 1H, isomer b), 4.78 (q, $J = 6.8$ Hz, 1H, isomer a), 2.31 (s, 3H, isomer a), 2.27 (s, 3H, isomer b), 1.71 (d, $J = 6.8$ Hz, 3H, isomer b), 1.67 (d, $J = 6.8$

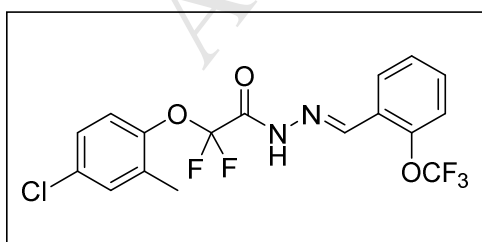
Hz, 3H, isomer a); ^{13}C NMR (100 MHz, CDCl_3) δ 173.0, 168.4, 153.7, 142.9, 132.0, 131.7, 131.3, 130.9, 129.6, 127.9, 127.4, 127.35, 127.3, 127.2, 127.1, 126.3, 126.2, 120.9, 114.8, 76.3, 71.5, 19.0, 18.1, 16.6, 16.4; HRMS (ESI-QTOF) m/z $[\text{M}+\text{H}]^+$ calcd for $\text{C}_{18}\text{H}_{17}\text{ClF}_3\text{N}_2\text{O}_3$ 401.0874, found 401.0873.

Compounds **8b-8c** were prepared by following the similar procedures as those for the synthesis of **8a**.



(E)-2-(4-Chloro-2-methylphenoxy)-2-methyl-N'-(2-(trifluoromethoxy)benzylidene)propanehydrazide (8b). White solid, mp: 175.8-178.2 °C; ^1H NMR

(400 MHz, CDCl_3) δ 9.93 (s, 1H), 8.42 (s, 1H), 8.21 (dd, $J = 1.2, 7.6$ Hz, 1H), 7.43 (t, $J = 7.0$ Hz, 1H), 7.33 (t, $J = 7.6$ Hz, 1H), 7.26 (m, 1H), 7.18 (d, $J = 2.0$ Hz, 1H), 7.05 (dd, $J = 2.4, 8.8$ Hz, 1H), 6.81 (d, $J = 8.8$ Hz, 1H), 2.26 (s, 3H), 1.61 (s, 6H); ^{13}C NMR (100 MHz, CDCl_3) δ 171.3, 151.2, 147.8, 142.3, 132.7, 131.8, 131.3, 128.4, 127.8, 127.3, 126.6, 126.4, 121.8, 121.0, 120.9, 119.2, 82.2, 25.3, 17.1; HRMS (ESI-QTOF) m/z $[\text{M}+\text{H}]^+$ calcd for $\text{C}_{19}\text{H}_{19}\text{ClF}_3\text{N}_2\text{O}_3$ 415.1031, found 415.1035.



(E)-2-(4-Chloro-2-methylphenoxy)-2,2-difluoro-N'-(2-(trifluoromethoxy)benzylidene)acetohydrazide (8c). White solid, mp: 167.4-170.2 °C; ^1H NMR (400

MHz, CDCl₃) δ 9.53 (s, 1H), 8.58 (s, 1H), 8.23 (d, J = 7.6 Hz, 1H), 7.51 (t, J = 7.0 Hz, 1H), 7.38 (t, J = 7.6 Hz, 1H), 7.30 (d, J = 8.0 Hz, 1H), 7.28-7.25 (m, 1H), 7.19 (s, 2H), 2.32 (s, 3H); ¹³C NMR (100 MHz, CDCl₃) δ 155.6, 155.2, 148.0, 146.0, 145.3, 133.4, 132.5, 132.1, 131.3, 127.9, 127.3, 127.0, 125.5, 123.4, 120.9, 114.6, 16.5; HRMS (ESI-QTOF) m/z [M+H]⁺ calcd for C₁₇H₁₃ClF₅N₂O₃ 423.0529, found 423.0527.

Stability in rat plasma

Ani9 or **5f** was incubated in rat plasma at a final concentration of 5 μ M for various incubation time (0, 30, 60, 120 and 240 min) at 37 °C shaking incubator. The reaction was terminated by three times volume of ice-cold acetonitrile and vortexed. The precipitated protein was removed by centrifugation at 13,000 RPM for 10 min. Supernatant was collected and analyzed by LC-MS/MS. Percentage of the parent compound remaining was calculated by comparing peak areas.

LC-MS/MS instrument and chromatographic separation

The HPLC system using Agilent 1200 series (Agilent Technologies, Santa Clara, CA, USA) with an API 4000 QTRAP triple quadrupole mass spectrometer (AB Sciex, Foster City, CA, USA) combined with a turbo electrospray interface was used for the quantitative analysis. The chromatographic separation was conducted by Kinetex C18 column (50 mm \times 2.1 mm i.d., 3 μ m; Phenomenex, USA) with a Security Guard C18 guard column (4 mm \times 20 mm i.d., Phenomenex, USA) and, the column was operated at a temperature of 35 °C. The mobile phase was consisted of 0.1% formic acid in water (eluent A) and 0.1% formic acid in ACN

(eluent B by isocratic elution (A:B=20:80, v/v) at a flow rate of 0.3 mL/min and run time was 3 min and injection volume of 5 μ L. The mass spectrometer was performed on multiple-reaction monitoring (MRM) mode by positive ionization condition. The most abundant product ions of compounds were 333.2 \rightarrow 161.2 for Ani9 and 387.1 \rightarrow 244.9 for **5f**. The optimized mass parameters were set as follow: ion spray voltage of 5500V; source temperature of 550 $^{\circ}$ C; curtain gas (CUR) of 30 psi; nebulizing gas (GS1) of 50 psi; heating gas (GS2) of 50 psi; collision energy (CE) of 31, 25 V, respectively.

Bioassay

Cell culture

Fisher rat thyroid (FRT) cells stably expressing ANO1 and ANO2 were established as described previously [31, 33]. FRT cells were cultured in Coon's modified F12 medium supplemented with 10% FBS, 2 mM L-glutamine, 100 units/mL penicillin and 100 μ g/mL streptomycin. PC3, MCF7 and BxPC3 cells were cultured in RPMI1640 medium containing 10% FBS, 100 units/ml penicillin and 100 μ g/ml streptomycin.

YFP fluorescence quenching assay

The FRT cells stably expressing YFP-H148Q/I152L/F46L and ANO1 or ANO2 were plated in 96-well plates at 2×10^4 cells per well and incubated for 48 hours. The 96-well plates were washed 3 times with 300 μ l PBS and 100 μ l PBS was left, and test compounds were applied at 20 minutes before the YFP fluorescence quenching assay. The 96-well plates were transferred to a microplate reader and fluorescence measurements were performed. To stimulate ANO1-mediated I $^{-}$ influx, 100 μ l of 70 mM I $^{-}$ solution containing 200 μ M ATP was

applied at 2 seconds, and the fluorescence was measured once every 0.4 second and continuously measured for 6 seconds. The inhibitory effect of the test compound was measured by calculating the initial slope of YFP fluorescence reduction by Γ influx. Assays were done using FLUOstar Omega microplate reader (BMG Labtech, Ortenberg, Germany) and MARS Data Analysis Software (BMG Labtech).

Ussing chamber study

Snapwell inserts containing FRT cells expressing ANO1, ANO2 or CFTR were placed in Ussing chambers (Physiologic Instruments, San Diego, CA). The basolateral bath was filled with HCO_3^- -buffered solution contained (in mM): 120 NaCl, 5 KCl, 1 MgCl_2 , 1 CaCl_2 , 10 D-glucose, 2.5 HEPES, and 25 NaHCO_3 (pH 7.4). Amphotericin B (250 $\mu\text{g}/\text{mL}$) was added to the basolateral bath for the selective permeabilization of basolateral membranes. The apical bath was filled with half Cl^- solution. The half Cl^- solution was prepared by replacing 65 mM NaCl with equimolar Na-gluconate in the HCO_3^- -buffered solution. The cells mounted on the bath were stabilized for 20 minutes and aerated with 95% O_2 / 5% CO_2 at 37 °C. Test compounds were added to the apical membrane for 20 minutes. Then, 100 μM ATP and 20 μM forskolin were added to the apical membrane to activate ANO1/2 and CFTR, respectively. Apical membrane currents were measured using an EVC4000 Multi-Channel V/I Clamp (World Precision Instruments, Sarasota, FL), and data were recorded using PowerLab 4/35 (AD Instruments, Castle Hill, Australia). Data collection and analysis were completed with Labchart Pro 7 (AD Instruments). The sampling rate was 4 Hz.

Cell viability assay

PC3, MCF7 and BxPC3 cells were plated in 96-well plate and incubated with 2% FBS

containing medium for 24 hours. When cells reached ~20% confluency, the cells were treated with Ani9, **5f**, and **5g** at 0.01, 0.03, 0.1, 0.3, 1, 3, 10 and 30 μM for 48 hours. The medium and compounds were exchanged every 24 hours. MTS assay was performed using the CellTiter 96® AQueous One Solution Cell Proliferation Assay kit (Promega, Madison, WI). Briefly, after removing the cell culture medium, MTS solution was added to the 96-well plate and reincubated for 1 hour. The absorbance of formazan was measured by Infinite M200 microplate reader (Tecan, Grödig, Austria) at 490 nm.

Western blot analysis

Western blotting was performed as described previously [31]. Briefly, PC3 cells were lysed with cell lysis buffer (50 mM Tris-HCl (pH 7.4), 1% Nonidet P-40, 150 mM NaCl, 1 mM EDTA, 0.25% sodium deoxycholate, 1 mM Na_3VO_4 , and protease inhibitor mixture). The whole cell lysates were centrifuged at 15000 g for 15 minutes at 4 °C and the supernatant protein was separated into 4-12% Tris-glycine precast gel (KOMA BIOTECH, Seoul, Korea). The protein was then transferred to PVDF membrane and then blocked with 4% non-fat skim milk in Tris-buffered saline contained in 0.1% Tween 20 (TBST) for 1 hour at room temperature. Subsequently, the membrane was reacted with primary ANO1 antibody (ab64085, 1:500, Abcam, Cambridge, MA), washed three times with TBST and reacted with goat anti-rabbit IgG secondary antibody (ADI-SAB-300-J, 1:2000, Enzo life science, New York, NY) for 1 hour at room temperature. The membrane was washed four times with TBST and it was visualized using the ECL Plus western blotting detection system (GE Healthcare, NJ).

Statistical analysis

The results of multiple experiments are presented as the means \pm S.E. Statistical analysis was performed with Student's t-test or by analysis of variance as appropriate. A value of $P < 0.05$ was considered statistically significant. Dose-response curve and IC_{50} values were calculated using GraphPad Prism Software.

Acknowledgements

This work was supported by the National Research Foundation of Korea (NRF) grant funded by the Korea government (MSIP) (NRF-2015R1D1A1A01057695 and 2017R1A2A2A05069364).

Supplementary data

^1H and ^{13}C NMR spectra of synthesized compounds.

References

- [1] C.R. Bader, D. Bertrand, R. Schlichter, Calcium-activated chloride current in cultured sensory and parasympathetic quail neurones, *J. Physiol.*, 394 (1987) 125-148.
- [2] W.A. Large, Q. Wang, Characteristics and physiological role of the Ca^{2+} -activated Cl^- conductance in smooth muscle, *Am. J. Physiol.*, 271 (1996) C435-454.
- [3] F. Huang, J.R. Rock, B.D. Harfe, T. Cheng, X. Huang, Y.N. Jan, L.Y. Jan, Studies on expression and function of the TMEM16A calcium-activated chloride channel, *Proc. Natl. Acad. Sci. U.S.A.*, 106 (2009) 21413-21418.
- [4] K. Kunzelmann, Y. Tian, J.R. Martins, D. Faria, P. Kongsuphol, J. Ousingsawat, F. Thevenod, E. Roussa, Rock, J. Schreiber R, Anoctamins, *Pflugers Arch.*, 462 (2011) 195-208.
- [5] U. Duvvuri, D.J. Shiwerski, D. Xiao, C. Bertrand, X. Huang, R.S. Edinger, JR. Rock, BD. Harfe, BJ. Henson, K. Kunzelmann, R. Schreiber, RS. Seethala, AM. Egloff, X. Chen, VW. Lui, JR. Grandis, SM. Gollin, TMEM16A induces MAPK and contributes directly to tumorigenesis and cancer progression, *Cancer Res.*, 72 (2012) 3270-3281.
- [6] W. Liu, M. Lu, B. Liu, Y. Huang, K. Wang, Inhibition of Ca^{2+} -activated Cl^- channel ANO1/TMEM16A expression suppresses tumor growth and invasiveness in human prostate

carcinoma, *Cancer Lett.*, 326 (2012) 41-51.

[7] A. Britschgi, A. Bill, H. Brinkhaus, C. Rothwell, I. Clay, S. Duss, M. Rebhan, P. Raman, CT. Guy, K. Wetzell, E. George, MO. Popa, S. Lilley, H. Choudhury, M. Gosling, L. Wang, S. Fitzgerald, J. Borawski, J. Baffoe, M. Labow, LA. Gaither, M. Bentires-Alj, Calcium-activated chloride channel ANO1 promotes breast cancer progression by activating EGFR and CAMK signaling, *Proc. Natl. Acad. Sci. U.S.A.*, 110 (2013) E1026-1034.

[8] Y. Li, J. Zhang, S. Hong, ANO1 as a marker of oral squamous cell carcinoma and silencing ANO1 suppresses migration of human SCC-25 cells, *Med. Oral Patol. Oral Cir. Bucal.*, 19 (2014) e313-319.

[9] J. Liu, Y. Liu, Y. Ren, L. Kang, L. Zhang, Transmembrane protein with unknown function 16A overexpression promotes glioma formation through the nuclear factor-kappaB signaling pathway, *Mol Med Rep.*, 9 (2014) 1068-74.

[10] Y. Sui, M. Sun, F. Wu, L. Yang, W. Di, G. Zhang, Z. Ma, J. Zheng, X. Fang, T. Ma, Inhibition of TMEM16A expression suppresses growth and invasion in human colorectal cancer cells, *PLoS One.*, 9 (2014) e115443.

[11] D.R.P. Sauter, I. Novak, S.F. Pedersen, E.H. Larsen, E.K. Hoffmann, ANO1 (TMEM16A) in pancreatic ductal adenocarcinoma (PDAC), *Pflugers Arch.*, 467 (2015) 1495-1508.

[12] F. Huang, H. Zhang, M. Wu, H. Yang, M. Kudo, C.J. Peters, PG. Woodruff, OD. Solberg, ML. Donne, X. Huang, D. Sheppard, J.V. Fahy, PJ. Wolters, BL. Hogan, WE. Finkbeiner, M. Li, YN. Jan, LY. Jan, JR. Rock, Calcium-activated chloride channel TMEM16A modulates mucin secretion and airway smooth muscle contraction, *Proc Natl Acad Sci U S A.*, 109 (2012) 16354-16359.

[13] H. Cho, Y.D. Yang, J. Lee, B. Lee, T. Kim, Y. Jang, SK. Back, HS. Na, BD. Harfe, F. Wang, R. Raouf, JN. Wood, U. Oh, The calcium-activated chloride channel anoctamin 1 acts as a heat sensor in nociceptive neurons, *Nat. Neurosci.*, 15 (2012) 1015-1021.

[14] A.S. Forrest, T.C. Joyce, M.L. Huebner, R.J. Ayon, M. Wiwchar, J. Joyce, N. Freitas, AJ. Davis, L. Ye, DD. Duan, CA. Singer, ML. Valencik, IA. Greenwood, N. Leblanc, Increased TMEM16A-encoded calcium-activated chloride channel activity is associated with pulmonary hypertension, *Am. J. Physiol.*, 303 (2012) C1229-C1243.

[15] B. Wang, C. Li, R. Huai, Z. Qu, Overexpression of ANO1/TMEM16A, an arterial Ca²⁺-activated Cl⁻ channel, contributes to spontaneous hypertension, *J. Mol. Cell. Cardiol.*, 82 (2015) 22-32.

[16] Y. Takayama, D. Uta, H. Furue, M. Tominaga, Pain-enhancing mechanism through interaction between TRPV1 and anoctamin 1 in sensory neurons, *Proc Natl Acad Sci U S A.*, 112 (2015) 5213-5218.

[17] F. Deba, B.F. Bessac, Anoctamin-1 Cl⁽⁻⁾ channels in nociception: activation by an N-aroylaminothiazole and capsaicin and inhibition by T16A[inh]-A01, *Mol Pain.* 2015 Sep 12;11:55

[18] J.S. Bae, J.Y. Park, S.H. Park, S.H. Ha, A.R. An, S.J. Noh, KS. Kwon, SH. Jung, HS. Park, MJ. Kang, KY. Jang, Expression of ANO1/DOG1 is associated with shorter survival and progression of breast

carcinomas, *Oncotarget.*, 9 (2018) 607-621.

[19] Y. Seo, K. Ryu, J. Park, D.K. Jeon, S. Jo, H.K. Lee, W. Namkung, Inhibition of ANO1 by luteolin and its cytotoxicity in human prostate cancer PC-3 cells, *PLoS One.*, 12 (2017) e0174935.

[20] Y. Seo, J. Park, M. Kim, H.K. Lee, J.H. Kim, J.H. Jeong, W. Namkung, Inhibition of ANO1/TMEM16A Chloride Channel by Idebenone and Its Cytotoxicity to Cancer Cell Lines, *PLoS One.*, 10 (2015) e0133656.

[21] A. Mazzone, S.T. Eisenman, P.R. Strege, Z. Yao, T. Ordog, S.J. Gibbons, G. Farrugia, Inhibition of cell proliferation by a selective inhibitor of the Ca(2+)-activated Cl(-) channel, Ano1, *Biochem. Biophys. Res. Commun.*, 427 (2012) 248-253.

[22] Y.D. Yang, H. Cho, J.Y. Koo, M.H. Tak, Y. Cho, W.S. Shim, SP. Park, J. Lee, B. Lee, BM. Kim, R. Raouf, YK. Shin, U. Oh, TMEM16A confers receptor-activated calcium-dependent chloride conductance, *Nature*, 455 (2008) 1210-1215.

[23] S. Pifferi, M. Dibattista, A. Menini, TMEM16B induces chloride currents activated by calcium in mammalian cells, *Pflugers Arch.*, 458 (2009) 1023-1038.

[24] P. Scudieri, E. Sondo, L. Ferrera, L.J. Galiotta, The anoctamin family: TMEM16A and TMEM16B as calcium-activated chloride channels, *Exp. Physiol.*, 97 (2012) 177-183.

[25] G.E. Ha, J. Lee, H. Kwak, K. Song, J. Kwon, S.Y. Jung, J. Hong, GE. Chang, EM. Hwang, HS. Shin, CJ. Lee, E. Cheong, The Ca(2+)-activated chloride channel anoctamin-2 mediates spike-frequency adaptation and regulates sensory transmission in thalamocortical neurons, *Nat. Commun.*, 7 (2016) 13791.

[26] G.E. Ha, E. Cheong, Calcium-activated chloride channels: a new target to control the spiking pattern of neurons, *BMB Rep.*, 50 (2017) 109-110.

[27] F. Neureither, K. Ziegler, C. Pitzer, S. Frings, F. Mohrlen, Impaired Motor Coordination and Learning in Mice Lacking Anoctamin 2 Calcium-Gated Chloride Channels, *Cerebellum.*, 16 (2017) 929-937.

[28] Y. Zhang, Z. Zhang, S. Xiao, J. Tien, S. Le, T. Le, LY. Jan, H. Yang, Inferior Olivary TMEM16B Mediates Cerebellar Motor Learning, *Neuron*, 95 (2017) 1103-1111.e1104.

[29] W. Namkung, P.W. Phuan, A.S. Verkman, TMEM16A inhibitors reveal TMEM16A as a minor component of calcium-activated chloride channel conductance in airway and intestinal epithelial cells, *J. Biol. Chem.*, 286 (2011) 2365-2374.

[30] S.J. Oh, S.J. Hwang, J. Jung, K. Yu, J. Kim, J.Y. Choi, HC. Hartzell, EJ. Roh, CJ. Lee, MONNA, a potent and selective blocker for transmembrane protein with unknown function 16/noctamin-1, *Mol. Pharmacol.*, 84 (2013) 726-735.

[31] Y. Seo, H.K. Lee, J. Park, D.K. Jeon, S. Jo, M. Jo, W. Namkung, Ani9, A Novel Potent Small-Molecule ANO1 Inhibitor with Negligible Effect on ANO2, *PLoS One.*, 11 (2016) e0155771.

[32] E.C. Truong, P.W. Phuan, A.L. Reggi, L. Ferrera, L.J.V. Galiotta, S.E. Levy, AC. Moises, O. Cil, E. Diez-Cecilia, S. Lee, AS. Verkman, MO. Anderson, Substituted 2-Acylaminocycloalkylthiophene-3-

carboxylic Acid Arylamides as Inhibitors of the Calcium-Activated Chloride Channel Transmembrane Protein 16A (TMEM16A), *J. Med. Chem.*, 60 (2017) 4626-4635.

[33] W. Namkung, J.R. Thiagarajah, P.W. Phuan, A.S. Verkman, Inhibition of Ca^{2+} -activated Cl^- channels by gallotannins as a possible molecular basis for health benefits of red wine and green tea, *FASEB J.*, 24 (2010) 4178-4186.

ACCEPTED MANUSCRIPT

Highlights

- Anoctamin 1 (ANO1), a calcium-activated chloride channel, is highly expressed and amplified in a number of carcinomas including breast, pancreatic and prostate cancers. Downregulation of ANO1 expression and function significantly inhibits cell proliferation, migration, and invasion of various cancer cell lines.
- A new class of ANO1 inhibitor, (*E*)-2-(4-chloro-2-methylphenoxy)-*N'*-(2-methoxybenzylidene)acetohydrazide (Ani9), has been discovered in our previous study.
- New Ani9 derivatives were designed and synthesized in order to identify more potent and selective ANO1 inhibitors.
- Structure-activity relationship studies with newly synthesized derivatives revealed **5f**, the most potent ANO1 inhibitor with an IC₅₀ value of 22 nM.
- The selectivity analyses revealed that **5f** has excellent selectivity to ANO1 (>1000-fold over ANO2). In cellular assays, **5f** significantly inhibited cell viability of PC3 (prostate cancer), MCF7 (breast cancer) and BxPC3 (pancreatic cancer) cells expressing high levels of ANO1. In addition, **5f** strongly reduced the level of ANO1 protein expression in PC3 cells.